

1.75
#8

Effects of Changes in an Alluvial
Channel on the Timing, Magnitude, and
Transformation of Flood Waves,
Southeastern Arizona

GEOLOGICAL SURVEY PROFESSIONAL PAPER 655-K



Effects of Changes in an Alluvial Channel on the Timing, Magnitude, and Transformation of Flood Waves, Southeastern Arizona

By D. E. BURKHAM

G I L A R I V E R P H R E A T O P H Y T E P R O J E C T

G E O L O G I C A L S U R V E Y P R O F E S S I O N A L P A P E R 6 5 5 - K



UNITED STATES DEPARTMENT OF THE INTERIOR

THOMAS S. KLEPPE, *Secretary*

GEOLOGICAL SURVEY

V. E. McKelvey, *Director*

Library of Congress Cataloging in Publication Data

Burkham, D. E., 1927-

Effects of changes in an alluvial channel on the timing, magnitude, and transformation of flood waves, southeastern Arizona.
(Gila River phreatophyte project)

(Geological Survey Professional Paper 655-K)

Bibliography: p. 24-25.

Supt. of Docs. no.: I 19.16:655-K

1. Gila River--Floods. 2. Channels (Hydraulic engineering) I. Title. II. Series: Gila River phreatophyte project. III. Series:
United States. Geological Survey Professional Paper 655-K.

QE75.P9 no. 655-K[TC425.G5]

557.3'08s[551.4'8]

75-619227

For sale by the Superintendent of Documents, U.S. Government Printing Office
Washington, D.C. 20402

Stock Number 024-001-02823-9

CONTENTS

	Page		Page
Abstract	K1	Temporal changes in spatial transformation of flood waves	K12
Introduction	1	Flood hydrographs	12
Characteristics of the study reach	3	Muskingum flood-routing method	17
Timing and velocity of flood waves	4	Basic concepts	17
Relation between peak discharge and lag time	4	Special methods	18
Comparisons of temporal changes in flood-wave lag time and		Routing of floods	19
velocity with changes in channel parameters	7	Floods of July 14-16, 1919, and September 3-5, 1925	19
Lag time	7	Flood of July 23-25, 1955	20
Velocity	7	Flood of January 11-17, 1960	21
Flow-boundary roughness	10	Discussion of results	21
Discussion of results	11	Summary and conclusions	22
		References cited	24

ILLUSTRATIONS

		Page
FIGURE 1.	Index map of project area and map showing study reach and location of gaging stations, Gila River	K2
2-11.	Graphs showing:	
	2. Relations between average peak discharge and lag time of the center of mass of flood waves moving through a reach of the Gila River	5
	3. Average peak discharge and differences in lag time of the center of mass of flood waves for four periods after 1927 compared with those for 1914-27	7
	4. Relations between average peak discharge and lag time of the peak-discharge rates of flood waves	8
	5. Annual floods, average stream-channel width, and lag time of center of mass of flood waves	9
	6. Historical changes in the bottom land in three reaches of the Gila River	10
	7. Average velocity of the center of mass of flood waves	11
	8. Measured and synthesized floodflow, July 14-16, 1919, and September 3-5, 1925	13
	9. Measured and synthesized floodflow, July 23-25, 1955	14
	10. Measured and synthesized floodflow, January 11-19, 1960	15
	11. Relation between inflow and outflow for peak discharges of floods moving through the study reach during 1914-27, 1930-32, and 1944-65	16

TABLES

		Page
TABLE 1.	Streamflow-gaging stations in or near Safford Valley	K3
2.	Velocity of the center of mass of flood waves and approximate values of Manning <i>n</i> for selected peak discharges	23

CONVERSION FACTORS

Factors for converting English units to the International System of Units (SI) are given below to four significant figures. However, in the text the metric equivalents are shown only to the number of significant figures consistent with the values for the English units.

<i>English</i>	<i>Multiply by</i>	<i>Metric</i>
acre-ft (acre-feet)	1233	m ³ (cubic metres)
ft (feet)	30.48	cm (centimetres)
ft (feet)3048	m (metres)
ft/s (feet per second)3048	m/s (metres per second)

CONTENTS

<i>English</i>	<i>Multiply by</i>	<i>Metric</i>
ft ³ /s (cubic feet per second) -----	0.02832 -----	m ³ /s (cubic metres per second)
mi (miles) -----	1.609 -----	km (kilometres)
mi ² (square miles) -----	2.590 -----	km ² (square kilometres)

GILA RIVER PHREATOPHYTE PROJECT

EFFECTS OF CHANGES IN AN ALLUVIAL CHANNEL ON THE TIMING, MAGNITUDE, AND TRANSFORMATION OF FLOOD WAVES, SOUTHEASTERN ARIZONA

BY D. E. BURKHAM

ABSTRACT

The stream channel of the Gila River in Safford Valley, Ariz., is wide and straight at the end of a period in which high flows have been dominant and is narrow and has a meander pattern at the end of a period in which low flows have been dominant; therefore, the size and meander pattern of the stream channel are regarded as determined by past dominant flows. The stream-channel and flood-plain system, when fully developed for a dominant flow, has a persistent effect on floods. A system developed for low flows reduces flood rates; the peak flows of flashy floods (floods that have large peak rates and small volumes) may be reduced to bankfull discharge. A system developed for high flows does not increase flood rates; however, streamflow from side tributaries along the study reach may contribute more significantly to peak rates in the Gila River when a high-flow system is in effect than when a low-flow system is in effect. At the downstream end of the study reach, the measured annual peak flows reflect the persistence of the upstream system and, therefore, are not random in time. A high-flow system was in effect during 1914–27, and a low-flow system began developing after about 1930 but was not fully developed until about 1964.

The velocity of the center of mass of flood waves that had peak discharges of between 10,000 and 20,000 ft³/s (cubic feet per second) or 283 and 566 m³/sec (cubic metres per second) during 1914–27 may have been up to three times as much as that for the same rates during 1943–70. During 1914–27, the trend was toward a gradual increase in velocity of the center of mass of flood waves—a decrease in lag time—as the peak discharge increased. During 1943–70, the trend was toward an increase in velocity of the center of mass of flood waves as the peak discharge increased from about 500 to 4,000 ft³/s (14 to 113 m³/s), a decrease in velocity as the peak discharge increased from about 4,000 to 20,000 ft³/s (113 to 566 m³/s) and an increase in velocity for a peak discharge of more than 20,000 ft³/s (566 m³/s). The velocities of the center of mass flood waves that had peak discharges of 300 to 500 ft³/s (8.5 to 14 m³/s) apparently were not significantly different for the two periods.

Outflow rates for flood waves moving through the study reach when the stream channel is wide and straight can be synthesized using the standard Muskingum flood-routing method (Carter and Godfrey, 1960) if an inflow hydrograph and an approximate value for the coefficient *K* are available. The standard Muskingum method, however, is not suitable for the routing of flood waves—except possibly for extremely small or large waves—that occur when the stream channel is narrow and the flood plain is fully developed.

INTRODUCTION

In the arid and semiarid regions of the United States, major changes in the width, depth, slope, meander pattern, and boundary material of several alluvial channels have been observed since about 1850 (Olmstead, 1919; Bryan, 1926; Schumm and Lichty, 1963; Burkham, 1972). The reasons for these changes have been described for a few channels (Schumm and Lichty, 1963; Burkham, 1972), but the adjustments in other components of the hydrologic system that were caused by these changes have not been described in any detail. Major channel changes probably will cause mutual adjustments in water and sediment yield, in the timing and magnitude of floods, in the surface-water and ground-water relations, and in vegetation types and density. A comprehensive knowledge of the temporal and spatial changes in all components of the hydrologic system is required before questions can be answered about the availability, distribution, and movement of water and the effects of human efforts to develop and control the water resources of arid and semiarid regions.

The Gila River in the semiarid Safford Valley in southeastern Arizona (fig. 1) is an example of an alluvial channel in which recent major changes in channel width, slope, meander pattern, and bottom-land vegetation have occurred (Burkham, 1972). This report gives descriptions of the effects on the timing, magnitude, and transformation of flood waves caused by changes in the Gila River in Safford Valley during 1914–70. The approach used in the study deals with lumped parameters, averages, and trends; this report advances general ideas derived from observations and reasonable speculations. Although adjustments in flood waves having peak discharges of more than about 10,000 ft³/s (283 m³/s) are of primary interest in this report, adjustments in smaller flood waves are described briefly.

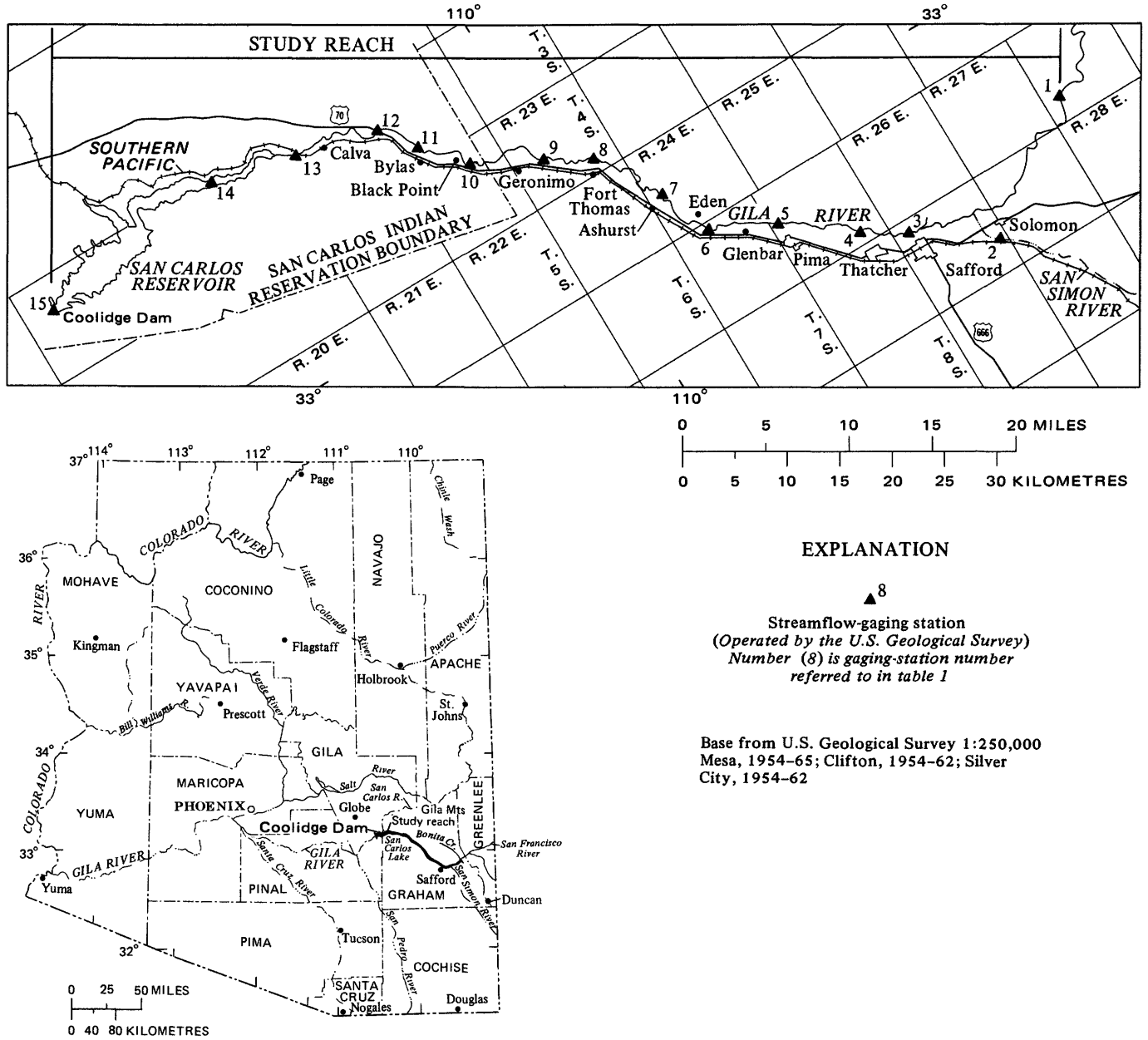


FIGURE 1.—Index map of project area and map showing extent of study reach and location of gaging stations, Gila River in Safford Valley.

The effects of channel changes on the timing, magnitude, and transformation of flood waves were determined by comparing temporal changes in lag time, velocity, and reservoir action with temporal changes in the size, shape, length, and tortuosity of the stream channel and in the vegetation on the flood plain. Lag time is the time required for a definable part of a flood wave to pass from the upstream end of a reach to the downstream end. Reservoir action refers to the modification of a flood wave by reservoir-type storage (Carter and Godfrey, 1960, p. 85). As used herein, the term "bottom land" refers to the area inundated during major

floods, and the term "flood plain" refers to the part of the bottom land not occupied by the stream channel. The term "stream channel" refers to the area that is generally void of vegetation and that has a definite bed in which flowing water is confined by banks.

Temporal changes in the lag time of flood waves were determined by comparing average relations between flood size and lag time and sets of inflow and outflow hydrographs for different time periods. Unless otherwise stated, the terms "lag time" and "lag time of the center of mass" refer to the time required for the center of mass of a flood wave to travel between two cross

sections of channel, and the term "lag time of the peak rate" refers to the time interval between the times that the peak rate of discharge of a flood wave occurs at the two cross sections.

Temporal changes in flood-wave velocity were determined from historical data for lag time and length of channel. The term "velocity of the center of mass" refers to the average velocity of the center of mass of a flood wave, and the term "velocity of the peak rate" refers to the average velocity of the peak discharge.

Temporal changes in reservoir action were determined by comparing sets of inflow and outflow hydrographs for different time periods. The significance of changes in timing of flood waves and reservoir action on flood routing was studied briefly using the Muskingum flood-routing method (Carter and Godfrey, 1960). Flood routing, which is the process of determining progressively the timing and magnitude of a flood wave at successive points along a river, was used as a tool in separating the attenuation effects of reservoir action on flood-peak rates from the attenuation effects of depletion of streamflow by infiltration.

Two principal types of data were used in this study—streamflow data and channel-change data. Streamflow records from 15 U.S. Geological Survey gaging stations in or near Safford Valley were used in the analyses (table 1; fig. 1). Most of the streamflow data used in the analyses are from the gaging stations Gila River at head of Safford Valley, near Solomon, Gila River at Calva, and Gila River at or near San Carlos (table 1; fig. 1). Data on channel changes are from a study made by Burkham (1972).

This report is one of several chapters of U.S. Geological Survey Professional Paper 655, which describes the environmental variables that affect evapotranspiration in the Gila River Phreatophyte Project area (Culler and others, 1970).

CHARACTERISTICS OF THE STUDY REACH

Safford Valley, which extends from the confluence of the Gila River and Bonita Creek to Coolidge Dam, is about 12 mi (19 km) wide and 75 mi (120 km) long (fig. 1). The valley is filled with more than 1,000 ft (300 m) of silt, sand, and gravel. The present (1972) stream channel of the Gila River in Safford Valley is from 60 to 800 ft (18 to 240 m) wide, and the bottom land area is from 1,000 to 5,000 ft (300 to 1,500 m) wide. The stream channel, a pool-and-riffle type, has an average slope of about 0.002. The depth to ground water in the alluvium along the river generally is less than 20 ft (6 m) below the land surface. Safford is at an altitude of 2,900 ft (880 m) above mean sea level in the upstream end of Safford Valley. The annual precipitation at Safford ranges from 3.0 to 17.5 in. (76 to 444 mm) and averages

TABLE 1.—Streamflow-gaging stations in or near Safford Valley

Plot No. (see fig. 2)	Gaging station	Period of record used in analysis
1	Gila River at head of Safford Valley, near Solomon	April 1914–September 1970
2	San Simon River near Solomon	June 1931–September 1932
	do	May 1935–September 1970
3	Gila River at Safford	June 1940–June 1947
	do	June 1948–June 1949
	do	October 1956–September 1965
4	Gila River near Thatcher ¹	June 1943–January 1944
5	Gila River at Pima ¹	July 1943–January 1944
6	Gila River near Glenbar ¹	June 1943–October 1944
7	Gila River near Ashurst ¹	June 1943–September 1944
8	Gila River at Fort Thomas ¹	July 1943–December 1944
9	Gila River near Geronimo ¹	June 1943–October 1944
10	Gila River at Black Point ¹	July 1943–October 1944
11	Gila River at Bylas ¹	June 1943–February 1944
12	Gila River near Bylas ²	October 1963–September 1970
13	Gila River at Calva	October 1929–September 1970
14	Gila River near Calva ²	February 1963–September 1970
15	Gila River at or near San Carlos ³	April 1914–October 1927

¹Gaging station was operated as a part of a study by Gatewood, Robinson, Colby, Hem, and Halpenny (1950). Data are in the files of the U.S. Geological Survey, Tucson, Ariz.

²Gaging station was operated as a part of a study by Culler and others (1970). Data are in the files of the U.S. Geological Survey, Tucson, Ariz.

³The completion of Coolidge Dam in 1928 made it necessary to relocate the downstream station from the "at or near San Carlos" site to the "at Calva" site.

about 8.7 in. (221 mm) (Sellers, 1960). The temperature extremes recorded at Safford are 7° and 114°F (−14° and 45.5° C) (Sellers, 1960).

The annual surface-water inflow for 1938–61 averaged about 257,000 acre-ft (317,000,000 m³) in the reach of the Gila River between the head of Safford Valley and Calva (Burkham, 1970a, table 4); the inflow includes 230,000 acre-ft (284,000,000 m³) that enters the reach at the head of Safford Valley gaging station. The annual flow at the Calva gaging station was about 145,000 acre-ft (179,000,100 m³) for 1938–61; therefore, the difference of 112,000 acre-ft (138,000,000 m³) was depletion by infiltration, evaporation, and diversions for irrigation. From November through June, streamflow is mainly from precipitation that falls during frontal storms, snowmelt, or outflow from ground-water storage and often is a combination of the three. About 70 percent of the flow in the Gila River at the head of Safford Valley occurs from November through June. The flow rate during November through June may be fairly constant for several days, and the sediment concentrations are relatively low. From July through October, streamflow is mainly from thunderstorms of small areal extent. The flow during July through October is usually flashy, and sediment concentrations generally are high.

The stream channel of the Gila River in Safford Valley changed significantly from 1846 to 1970 (Burkham, 1972). From 1846 to 1904 the channel meandered through a flood plain covered with willow, cottonwood, and mesquite. The average width of the channel was less than 150 ft (45 m) in 1875 and less than 300 ft (90 m) in 1903. During 1905–17, large winter floods caused major destruction in the flood plain, and the average width of the channel increased to about 2,000 ft (600 m).

At the head of Safford Valley, most of the destructive

floods during 1905–17 originated in mountainous terrain, which does not erode easily. Therefore, the amount of sediment supplied to the reach was less than the river could carry at full debris-carrying capacity—the maximum load a flood is capable of carrying (Rubey, 1937). The alluvial deposits in Safford Valley in 1905–17 were formed primarily of easily eroded sediment. Reconstruction of the flood plain was underway during 1918–70; the stream channel narrowed, and the average width was less than 200 ft (60 m) in 1964. The flood plain became densely covered with saltcedar during 1918–70. Minor widening of the stream channel occurred as a result of the large floods in 1941, 1965, and 1967, and the average width of the channel was about 400 ft (120 m) in 1968.

The period of flood-plain reconstruction was characterized by floods having low peak discharges relative to those in 1905–17 and large sediment loads relative to the debris-carrying capacity of the Gila River during 1918–70 (Burkham, 1972). Primarily, the large sediment loads came from the rapid erosion of alluvial deposits in the low-altitude drainage basins tributary to the Gila River. The small floods that originated in these tributary basins spread over the wide channel of the Gila River, lost kinetic energy, and deposited their sediment. During 1935–70 the average rate of aggradation along the bottom land was 0.03 ft/yr (0.91 cm/yr) in the reach from the confluence of the Gila and San Simon Rivers to the bridge at Pima and 0.08 ft/yr (2.44 cm/yr) in the reach from the bridge at Pima to the east boundary of the San Carlos Indian Reservation. The dense cover of saltcedar and the cultivation of the bottom land may have contributed significantly to the rapid reconstruction of the flood plain.

The rapid erosion in the low-altitude drainage basins tributary to the Gila River apparently was triggered by the large floods of 1905–17 (Burkham, 1972). The widening of the stream channel of the Gila River decreased the length of most of the tributary streams at their confluences with the Gila River and increased the gradients of the tributaries near the confluences. The increased gradients and the large floods started severe erosion in the tributary streams at their confluences with the Gila River. Soon deep channels were eroded near the Gila River; these deep channels eventually became wide and extended far upstream (Burkham, 1972).

TIMING AND VELOCITY OF FLOOD WAVES

The timing and velocity of flood waves are dependent on other factors in addition to the channel parameters—size, shape, slope, roughness, and bed forms. For example, the timing and velocity of floods in the study reach are dependent on the size and shape of

the inflow waves, on the debris carried by the flood, and on the loss of surface water within the valley. All these parameters change continually with time and place along the Gila River. Data are not adequate to evaluate the reasons for all the changes; however, rational speculation about reasons for the average long-term changes or trends is possible. The average relations between lag time and magnitude of flood waves for different time periods were established in order to determine the average temporal changes in the timing and velocity of flood waves of different magnitudes. The temporal changes in the timing and velocity of flood waves then were correlated with temporal channel changes of the Gila River. Water loss affects both lag time and size of flood wave; hopefully, bias in the relations between lag time and flood-wave magnitude is minimized by using an average peak discharge for the flood-magnitude variable.

In the following sections the lag time of the center of mass of flood waves is discussed in detail, and the lag time of peak discharge is discussed briefly. The date for a particular flood is the date of arrival of the flood at the upstream end of the study reach.

RELATION BETWEEN PEAK DISCHARGE AND LAG TIME

Graphs showing the relation between average peak discharge and lag time of the center of mass of flood waves are based on data for five time periods: 1914–27, 1930–40, 1941–50, 1951–60, and 1961–70 (fig. 2). The inflow rates for 1914–70 measured at the head of Safford Valley gage, the outflow rates for 1914–27 measured at the San Carlos gages, and the outflow rates for 1930–70 measured at the Calva gage were used in developing the relations. The inflow and outflow data are for storm periods when the tributary inflow to the study reach was an insignificant part of the outflow. The times when the center of mass of a flood wave passed the ends of the study reach were needed to determine the lag time; the times used were when half of the total volume of the wave had passed the gaging stations. The average peak discharge for a flood moving through the study reach was computed using the equation

$$Q_p = \frac{I_p + O_p}{2} \quad (1)$$

in which

- Q_p = average peak discharge;
- I_p = peak inflow; and
- O_p = peak outflow.

The data for average peak discharge and lag time of the center of mass for the period 1914–27 were adjusted before being plotted in figure 2 because the 1914–27 data are for the reach from the Solomon gaging station

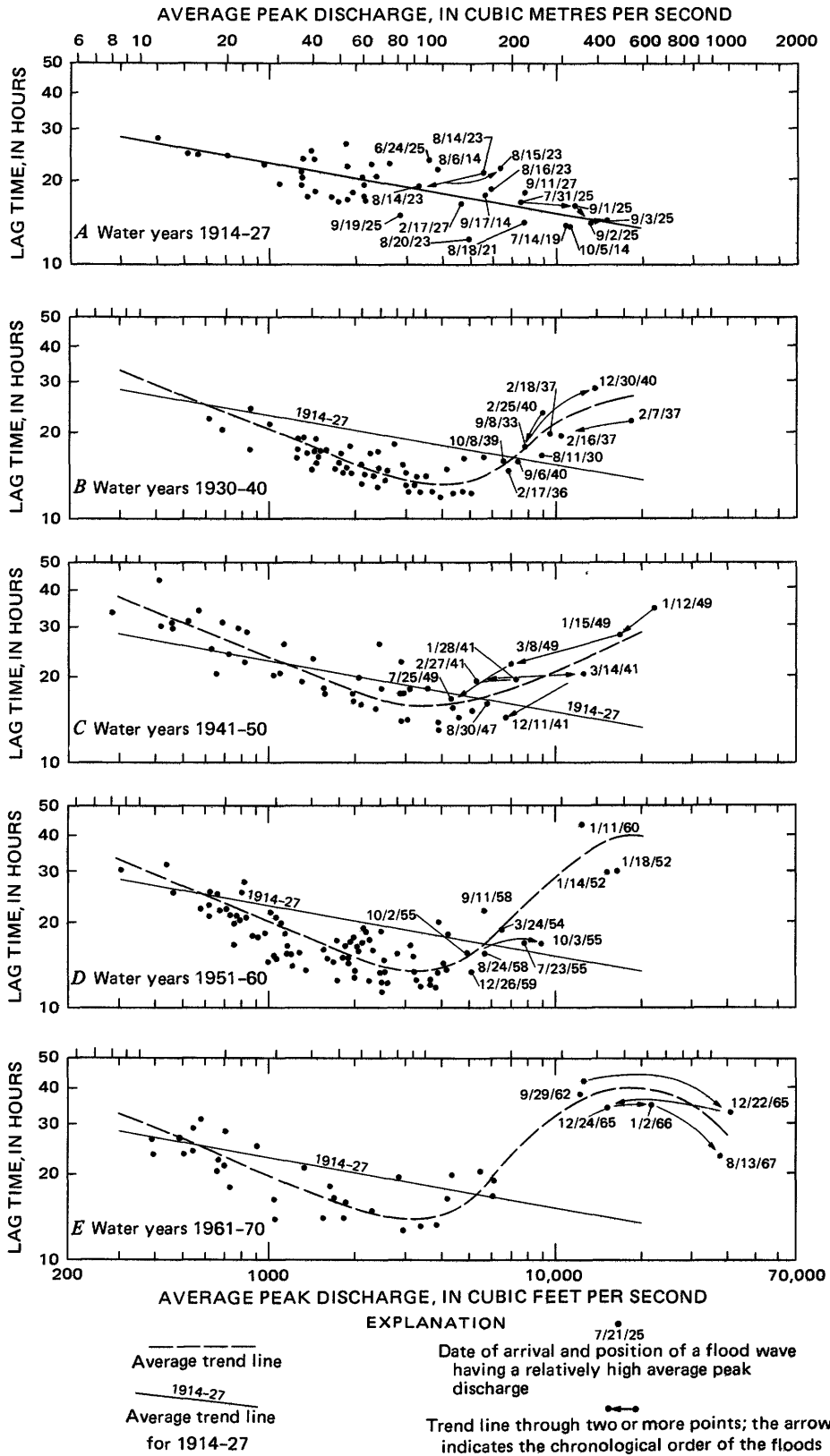


FIGURE 2.—Relations between average peak discharge and lag time of the center of mass of flood waves moving through a 55-mile (88 km) reach of the Gila River in Safford Valley. Average peak discharge for a flood wave was taken as the mean of the peak rates at the ends of the reach.

to the San Carlos gaging station, which is 71 mi (114 km) long, whereas the data for the other periods are for the reach from the Solomon gaging station to the Calva gaging station, which is 55 mi (88 km) long (fig. 1). Each lag time was adjusted by multiplying it by the ratio 55/71. For lack of a better method, the adjusted data for average peak discharge for 1914–27 were obtained using the equation

$$Q_p = I_p + \frac{(O_p - I_p)}{2} (55/71). \quad (2)$$

The average trend lines in the graphs in figure 2 are approximations of average changes in lag time as the average peak discharge varied. The large scatter in data points probably is a direct result of unstable channel and flood-plain conditions, and of water loss along the channel.

The trend during 1914–27 was toward a gradual decrease in lag time as the average peak discharge increased (fig. 2A); the trend is indicative of flow in which the external resistance to water movement is mainly from the channel bottom. Most flood waves during the period spread over a flood channel that was about 2,000 ft (600 m) wide, fairly flat in cross section, straight, and relatively free of vegetation (Burkham, 1972). The large scatter of data points about the trend line in figure 2A may have resulted from differences in bedforms in the channel, in sizes of sediment in the flow and along the channel, and in the degree of flood-plain development.

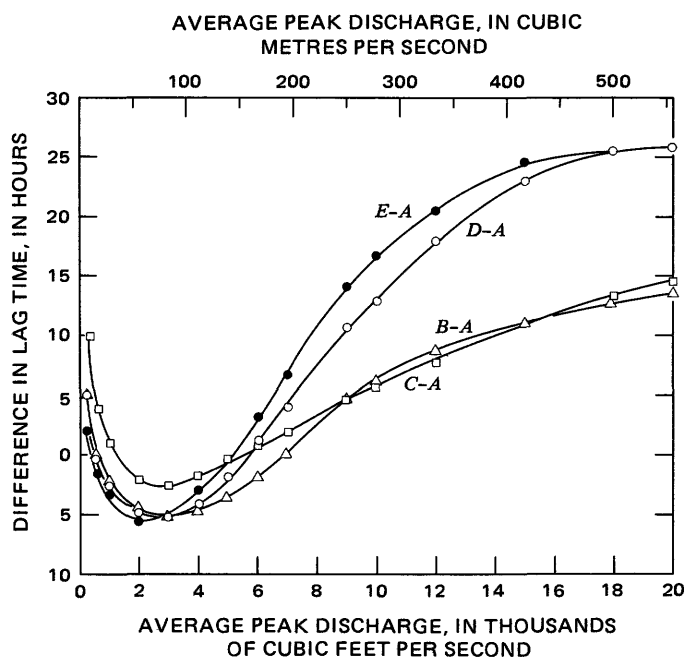
After 1930, the trend apparently was toward a decrease in lag time as the average peak discharge increased from about 300 to 3,000 ft³/s (8.5 to 85 m³/s) and an increase in lag time as the average peak discharge increased from about 5,000 to 20,000 ft³/s (142 to 566 m³/s) (fig. 2). The minimum lag times shown by the different average trend lines for periods after 1927 ranged from 13 to 16 hours for flood waves with average peak discharges of 3,000 to 5,000 ft³/s (85 to 142 m³/s). The lag time taken from the average trend line for 1914–27 was about 18 hours for flood waves with the same discharge. Therefore, the decrease in lag time after about 1927 for flows of 3,000–5,000 ft³/s (85–142 m³/s) is assumed to be about 10 to 30 percent. Flood waves that had average peak discharges of 10,000 to 20,000 ft³/s (283 to 566 m³/s) apparently had lag times which averaged about 14 to 16 hours in 1914–27, 20 to 30 hours in 1930–50, and 30 to 40 hours in 1951–70.

The minimum lag time shown by the trend lines for the different periods after 1927 was assumed to have occurred at about bankfull discharge (Linsley and others, 1949), corresponding to the stage at which water moves onto the flood plain. Based on discharge measurements made at different times at several sites along

the study reach, the velocity of shallow flow on the densely vegetated flood plain is significantly less than the velocity of bankfull flow in the stream channel. Because of this difference, a change in the slope of the discharge-to-lag time relation should occur at about bankfull discharge; the change should be toward a longer lag time as the discharge increases. For the four periods after 1927, changes in the slope of the average discharge-to-lag-time relations occur at average peak discharges ranging from 3,000 to 5,000 ft³/s (85 to 142 m³/s). The bankfull discharge for short reaches near Calva, Ariz., for 1962 and 1963 was determined to be about 4,000 ft³/s (113 m³/s) (Burkham and Dawdy, 1970; Culler and others, 1970). However, the range in bankfull discharge along the reach for a given time and the range at a given site for the period 1927–70 are probably significantly different.

The maximum lag time for large flood waves moving through the study reach in 1960–70 apparently occurred when the average peak discharge was about 20,000 ft³/s (566 m³/s); this assumption is based on data from floods in January 1960, September 1962, December 1965, January 1966, and August 1967 (fig. 2). The lag times for the flood waves of January 11, 1960, and September 29, 1962, that had average peak discharges of 12,000 to 13,000 ft³/s (340 to 368 m³/s) were from 38 to 42 hours; the trend in the relation of average peak discharge to lag time at these rates apparently is toward an increase in lag time with an increase in peak discharge. The lag time for the flood wave of December 22, 1965, that had an average peak discharge of about 40,000 ft³/s (1,130 m³/s), however, was only about 32 hours, and the trend in the relation of average peak discharge to lag time apparently is toward a decrease in lag time with an increase in discharge. The lag-time data for the three floods seem to indicate that a maximum lag time is reached for floods that have average peak discharges of 15,000 to 25,000 ft³/s (425 to 705 m³/s); the same conclusion can be reached by studying the lag-time data for the flood waves of December 1965, January 1966, and August 1967. The lag time for the August 1967 flood wave, however, may have been reduced slightly as a result of the eradication of bottomland vegetation in 1967 in the 5.5-mi (8.8 km) reach of the channel from the gaging station near Bylas to the gaging station at Calva (Burkham, 1976).

The relations between average peak discharge and differences in lag time for the four periods after 1927 are compared with those for 1914–27 in figure 3. The discharge with the maximum negative difference in lag time is about bankfull discharge; a negative difference indicates a decrease in lag time. The reason for the increase in lag times for flood waves having average peak discharges from 300 to 500 ft³/s (8.5 to 14 m³/s)



EXPLANATION



The difference in lag time was computed by subtracting the lag time obtained from curve *A* from the lag time from curve *E* in figure 2. Curve *A* in figure 2 is for the period 1914-27; curve *B* is for the period 1930-40; curve *C* is for the period 1941-50; curve *D* is for the period 1951-60; and curve *E* is for the period 1961-70. A positive difference indicates an increase in lag time

FIGURE 3.—Average peak discharge and differences in lag time of the center of mass of flood waves for four periods after 1927 compared with those for 1914-27.

apparently is largely due to an increase in channel length caused by an increase in stream-channel meander. The effects of channel meander on changes in lag time are discussed further in the section "Comparisons of Temporal Changes in Flood-Wave Lag Time and Velocity with Changes in Channel Parameters."

As expected, the trends in the relation of average peak discharge to lag time of the peak rate roughly parallel the trends in the relation of average peak discharge to lag time of the flood wave; however, a few differences were noted (figs. 2, 4). For example, the average peak discharge with the minimum peak-rate lag time for the two periods after 1950 apparently is smaller than the average peak discharge with the minimum center-of-mass lag times. Also, the scatter of data points on the different peak-lag diagrams is greater than the scatter on the corresponding mass-lag diagrams. The reasons for these differences are not known.

The peak-rate lag time, however, is known to be more susceptible to changes in the spatial factors that control water movement than the center-of-mass lag time, which probably accounts for most of the difference in the scatter of plotted data. Because of the smaller scatter of plotted points, the average peak discharge corresponding to the minimum lag time shown by the different mass-lag relations is assumed to be a better estimate of the bankfull discharge for the two periods after 1950 than that shown by the peak-lag relation.

COMPARISONS OF TEMPORAL CHANGES IN FLOOD-WAVE LAG TIME AND VELOCITY WITH CHANGES IN CHANNEL PARAMETERS

LAG TIME

The temporal increase after 1927 in lag time for flood waves that had average peak rates greater than bankfull discharge apparently was caused by the narrowing of the stream channel, development of a meander pattern, development of a flood plain, and growth of flood-plain vegetation (figs. 5, 6). Abrupt decreases in lag time, however, apparently follow major floods that widen and straighten the stream channel (fig. 5). The large flood of December 22, 1965, undoubtedly caused a reduction in lag times for the flood waves of December 24, 1965, January 2, 1966, and August 13, 1967. As previously discussed, the lag time of the flood wave on August 13, 1967, also may have been affected by the eradication of bottom-land vegetation along 5.5 mi (8.8 km) of channel near the downstream end of the study reach.

The length of the main path of flow (L) may have been an important factor in changes in lag time for some flows. Lag times vary with L , which in the study reach changes with time and discharge. For example, most of the flow during floods that occurred during this study moved directly downvalley, and L for these flows was about 55 mi (88 km)—the length of the study reach. Flood waves that had averaged peak discharges of less than about 5,000 ft³/s (142 m³/s), however, followed the meandering stream channel, and L increased from about 55 mi (88 km) in 1918 to about 66 mi (106 km) in 1964 for these floods (Burkham, 1972).

VELOCITY

The velocity of the center of mass of flood waves that had average peak discharges of 300 to 500 ft³/s (8.5 to 14 m³/s) apparently did not change greatly between the 1914-27 and 1961-70 periods. The average velocity of the center of mass was obtained by dividing the length of the main flow path by lag time. The length of the main flow path (L) and the lag time (T_m) used to compute the velocity were 55 mi (88 km) and 26 to 28 hours for

GILA RIVER PHREATOPHYTE PROJECT

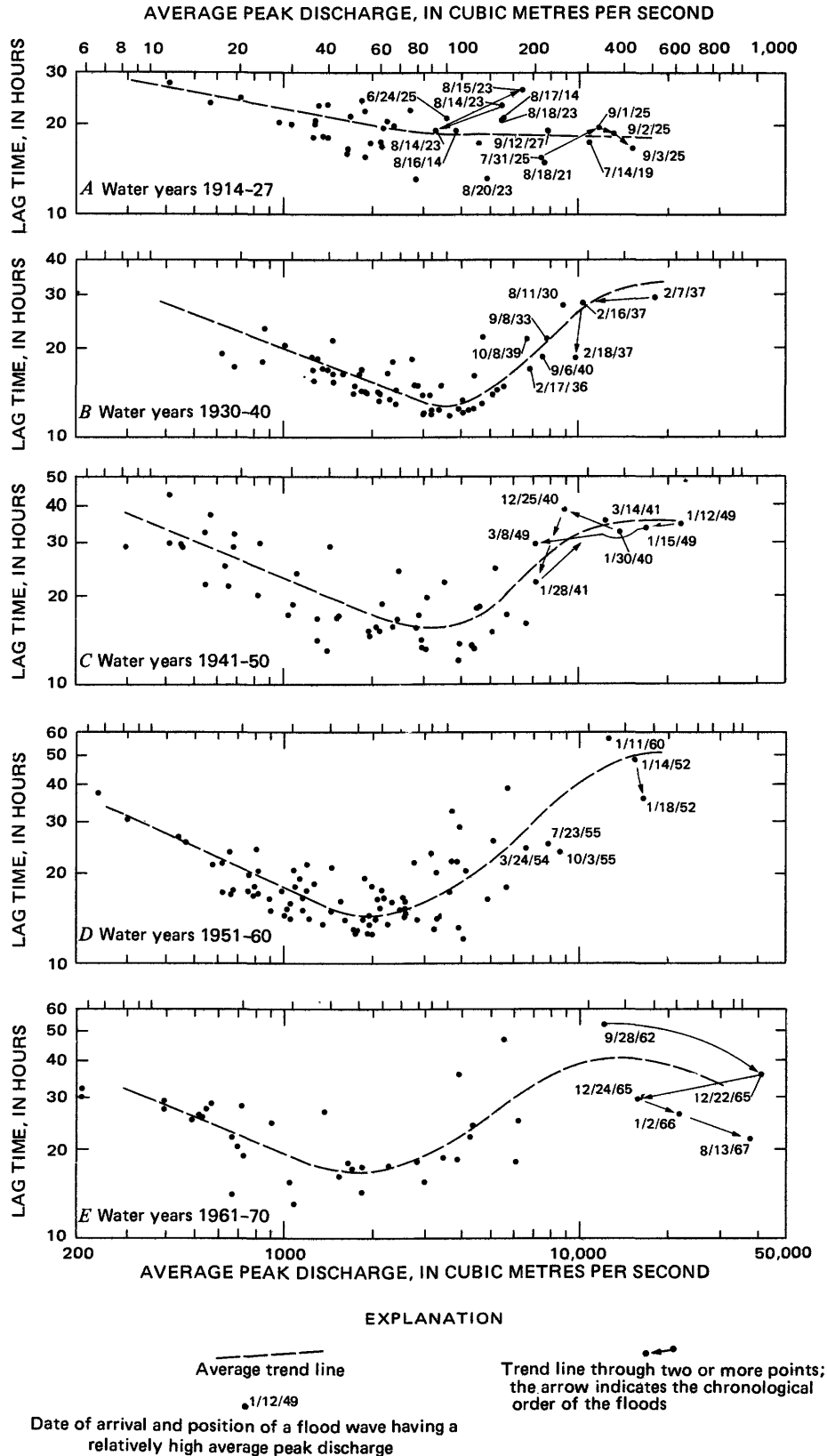
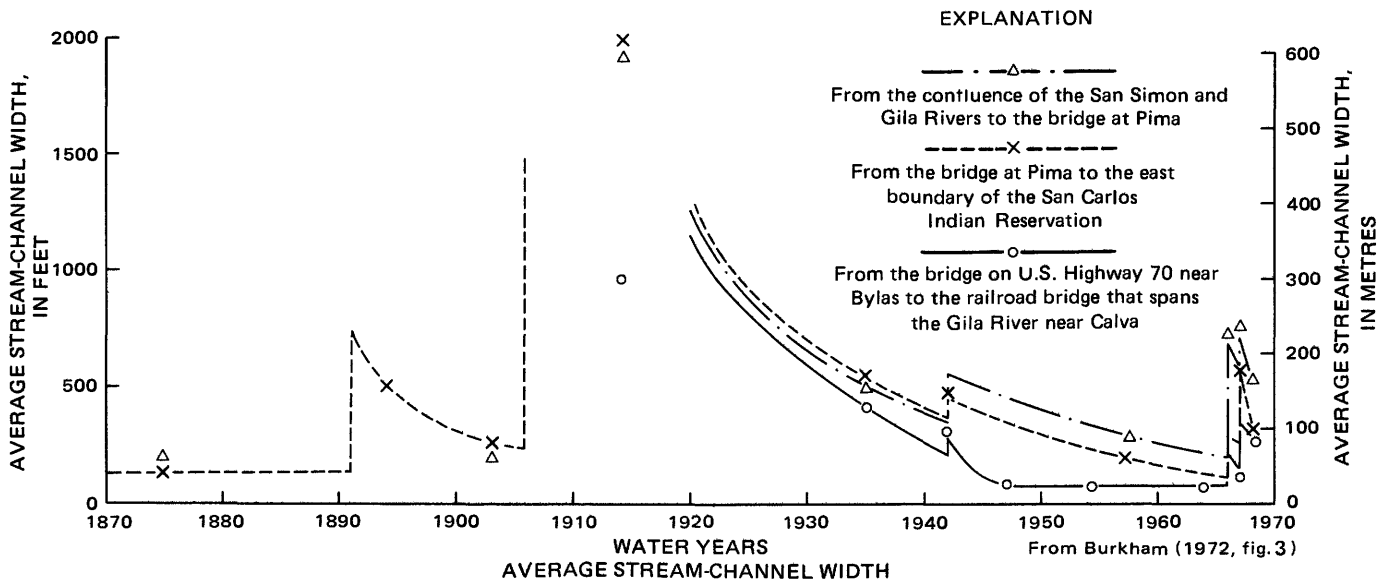
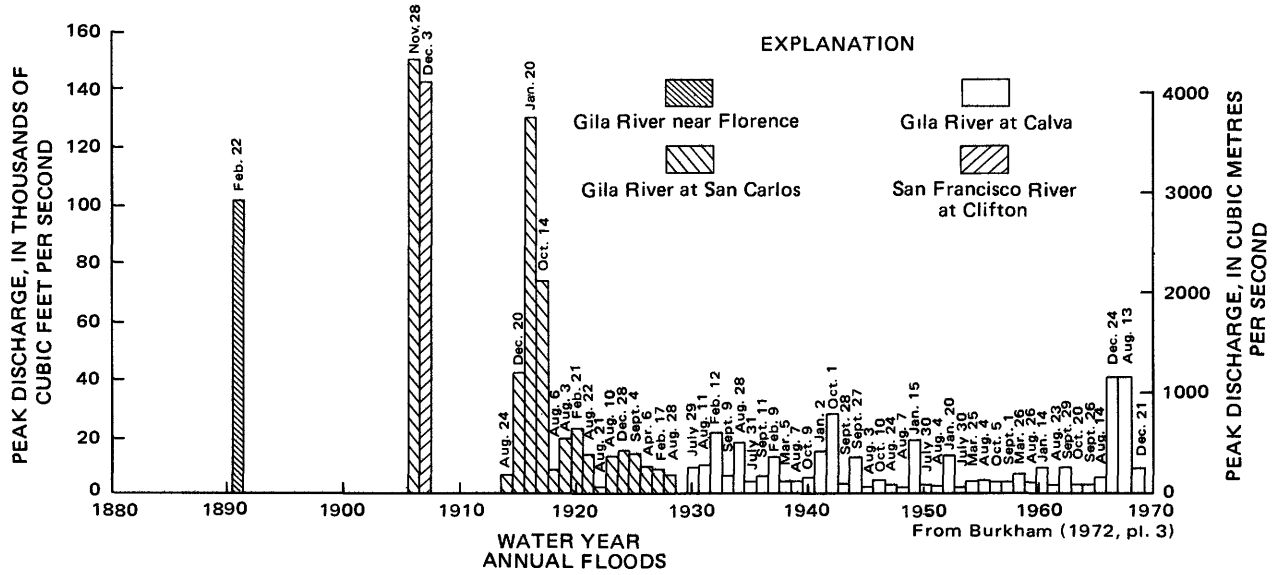


FIGURE 4.—Relations between average peak discharge and lag time of the peak-discharge rates of flood waves moving through a 55-mi (88 km) reach of the Gila River in Safford Valley. Average peak discharge for a flood wave was taken as the mean of the peak rates at the ends of the reach.



NOTE: Lag-time data are for the 55-mile (88.5-kilometre) reach from the gaging station near Solomon to the gaging station at Calva (fig. 1)

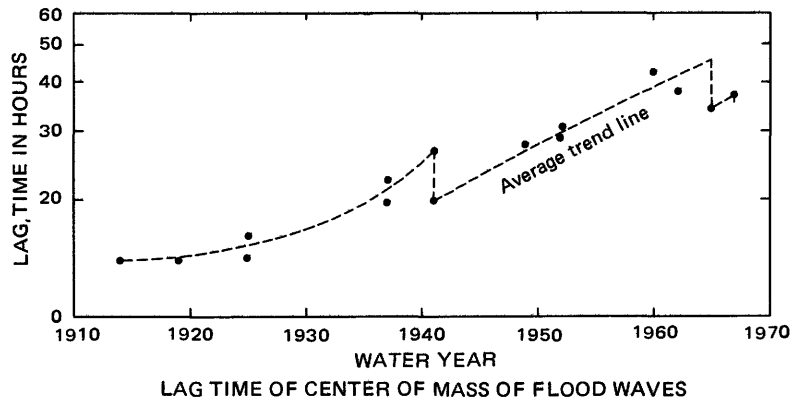


FIGURE 5.—Annual floods, average stream-channel width, and lag time of center of mass of flood waves having average peak discharges of 10,000–20,000 ft³/s (283 to 566 m³/s), Gila River in Safford Valley. Average peak discharge of flood wave was taken as the mean of the peak rates at the ends of the reach.

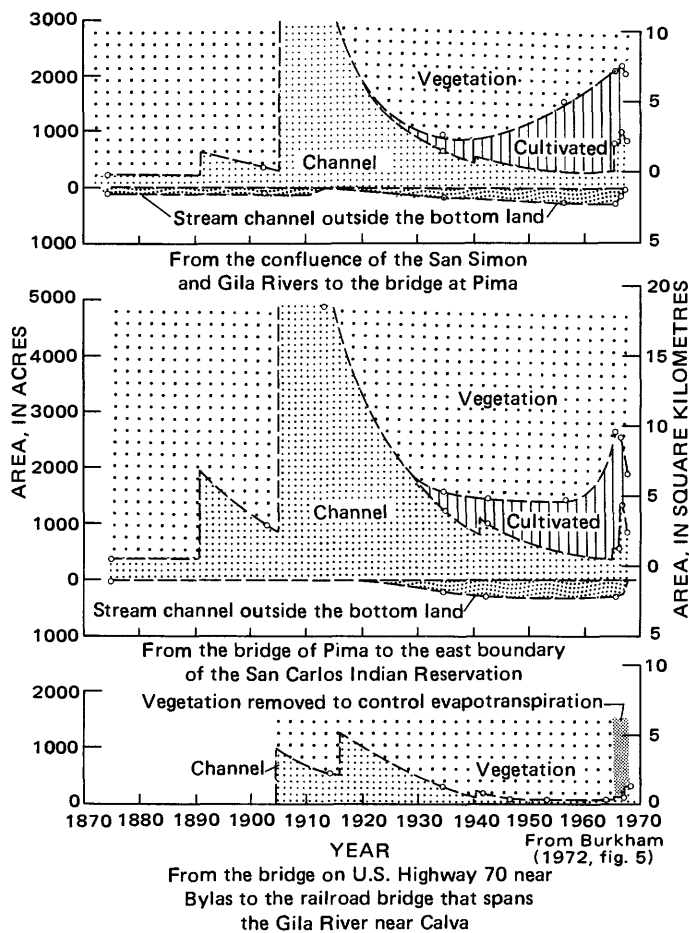


FIGURE 6.—Historical changes in the bottom land in three reaches of the Gila River in Safford Valley.

1914–27, and 66 mi (106 km) and 28 to 33 hours for 1964–70; lag times were taken from the trend lines shown in figure 2. The velocity of the center of mass of flood waves that had average peak discharges of 300 to 500 ft³/s (8.5 to 14 m³/s) was about 2.9 to 3.1 ft/s (0.88 to .94 m/s) during 1914–27 and 2.9 to 3.4 ft/s (0.88 to 1.04 m/s) during 1961–70. The increase in lag time for these peak-flow rates, therefore, apparently was due to the increase in length of channel because the average velocity for 1961–70 was not significantly different from the average velocity for 1914–27.

The velocity of the center of mass of flood waves that had average peak discharges of 3,000 to 5,000 ft³/s (85 to 142 m³/s) was about 4.2 to 4.7 ft/s (1.3 to 1.4 m/s) during 1914–27 and 6.0 to 6.9 ft/s (1.8 to 2.1 m/s) in 1961–70. The values of L and T_m used to compute the velocity were 55 mi (88 km) and 17 to 19 hours for 1914–27 and 66 mi (106 km) and 14 to 16 hours for 1961–70; the lag times were taken from the trend lines shown in figure 2. The increase in velocity between 1914–27 and 1961–70 for flood waves that had average peak discharges of

3,000 to 5,000 ft³/s (85 to 142 m³/s) apparently resulted from narrowing of the stream channel.

Temporal changes in the velocity of the center of mass of flood waves that had average peak discharges of 10,000 to 20,000 ft³/s (283 to 566 m³/s) are shown in figure 7. The plotted velocities were computed using a value of 55 mi (88 km) for L and values obtained from the trend line in figure 5 for T_m . The velocity of flood waves that had average peak discharges of 10,000 to 20,000 ft³/s (283 to 566 m³/s) during 1914–18 apparently was more than three times that for the same rates in 1964.

FLOW-BOUNDARY ROUGHNESS

Most of the changes in the lag time and velocity of flood waves that had peak discharges of more than 5,000 ft³/s (142 m³/s) undoubtedly resulted from changes in flow-boundary roughness—roughness of the stream channel and flood plain. A precise method for evaluating average temporal changes in lag time caused by changes in flow-boundary roughness for rapidly varied unsteady flows in the reach was not available for this study. However, discussions of changes in roughness, as represented by the Manning roughness coefficient n , and the effects of these changes are presented. The Manning equation is

$$V = \frac{1.49}{n} R^{2/3} S^{1/2}, \quad (3)$$

in which

- V = mean velocity of flow at a cross section;
- R = hydraulic radius at a cross section;
- S = energy gradient; and
- n = roughness coefficient.

The Manning equation was developed for uniform flow, in which the water-surface profile and energy gradient are parallel to the streambed, and the area, hydraulic radius, and depth remain constant throughout the reach. The equation is considered valid for nonuniform flow, such as that of the Gila River, if the energy gradient or friction slope is modified to reflect only the losses due to boundary friction (Barnes, 1967, p. 4). The equation is considered valid, however, only for flow in relatively short reaches (Dalrymple and Benson, 1967).

In this study, the Manning roughness coefficient, n , is treated as a lumped parameter, and its value during flow in an alluvial channel and flood plain depends on a number of time-variant and space-variant factors. Some of the factors in the study reach that probably exert the greatest influence on the coefficient of roughness for flows greater than about 5,000 ft³/s (142 m³/s) are (1) flow-boundary roughness, (2) size and shape of stream

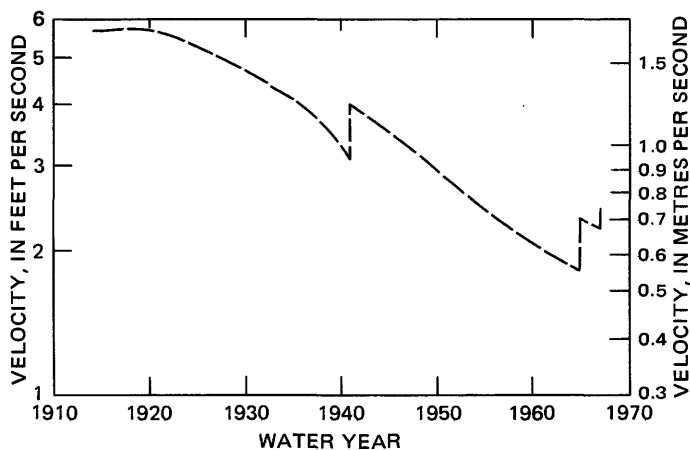


FIGURE 7.—Average velocity of the center of mass of flood waves that had average peak discharges of 10,000 to 20,000 ft^3/s (283 to 566 m^3/s) for 1914–70, Gila River in Safford Valley. Average peak discharge of a flood wave was taken as the mean of the peak rates at the ends of the reach. Velocity was taken as the ratio of the length of the main flow path (55 mi, 88 km) divided by the lag time of the center of mass of the flood wave; the lag time was obtained from the trend lines shown in figure 5.

channel and flood plain, (3) stream-channel irregularity and alinement, (4) vegetation, (5) obstructions, (6) flow depth and rate, (7) filling and scouring, (8) size and concentration of sediment in flow, and (9) bed forms. Most of these factors are interdependent. Factors 1 to 5 are known to have changed significantly during 1914–70 (Burkham, 1972). The changes, in general, have been in a direction that would increase the roughness coefficient. The relative influence of bed-form roughness probably decreased as stream-channel width decreased and as the density of vegetation on the flood plain increased.

The roughness coefficient n for most of the study reach for most floods during 1914–27 probably ranged between 0.02 and 0.04. This estimate of the probable range in n is based on photographs and other data (Olmstead, 1919; Burkham, 1972). C. C. Jacob (U.S. Geological Survey, written commun., 1916) collected data for 1916 flow rates greater than 25,000 ft^3/s (705 m^3/s); these data were used to compute n values for short reaches at the upstream and downstream ends of Safford Valley. The n values obtained using Jacob's data in equation (3) were 0.024 and 0.027.

The average roughness coefficient for most of the study reach for flows ranging from about 300 to 5,000 ft^3/s (85 to 142 m^3/s) probably ranged from 0.02 to 0.04 during 1914–70; for flows ranging from 10,000 to 40,000 ft^3/s (283 to 1,130 m^3/s), the value of n probably ranged from 0.06 to 0.14 for most of the study reach during the same period. These estimates of the probable range in n are based on photographs and other data (Burkham,

1972) and on the author's observations and studies. The author made several preliminary evaluations for n using equation (3) for 1962–70 flows below bankfull discharge at nine cross sections in the 15-mi (24-km) study reach of the Gila River Phreatophyte Project area (Culler and others, 1970); the roughness coefficient n ranged from 0.02 to 0.04. In making the evaluations the velocity and hydraulic radius in equation (3) were known, and S was assumed to be equal to the slope of the water surface. The average value of n computed for selected reaches in the Gila River Phreatophyte Project area (Culler and others, 1970) for peak flows of 39,000 and 40,000 ft^3/s (1,100 and 1,130 m^3/s)—which occurred in 1965 and 1967, respectively—was about 0.08 (Burkham, 1976).

DISCUSSION OF RESULTS

The lack of major floods in the study reach during 1918–64 led to channel changes that greatly affected the lag time and velocity of floods. The wide stream channel that existed in 1914 changed: the stream channel became narrower, stream-channel meander increased, natural levees developed along the stream channel, flood-plain vegetation spread and became dense, and large alluvial fans developed at the mouth of tributaries (Burkham, 1972). In addition, cultivation of the flood plain increased during the absence of large floods. After the changes, the Gila River consisted of a stream channel in which flow below bankfull discharge—3,000 to 5,000 ft^3/s (85 to 142 m^3/s) after 1930—moved relatively fast and a congested flood plain in which floodflow moved relatively slow. The velocity of the center of mass of flood waves that had average peak discharges of 300 to 500 ft^3/s (85 to 142 m^3/s) apparently did not change greatly during 1914–70; the velocity was about 2.9 to 3.1 ft/s (0.88 to 0.94 m/s) during 1914–27 and 2.9 to 3.4 ft/s (0.88 to 1.04 m/s) during 1961–70. The range in velocity of the center of mass of flood waves that had average peak discharges of 3,000 to 5,000 ft^3/s (85 to 142 m^3/s), however, increased from 4.2 to 4.7 ft/s (1.28 to 1.43 m/s) during 1914–27 to 6.0 to 6.9 ft/s (1.83 to 2.10 m/s) during 1961–70. The increase during 1914–70 in velocity of flood waves that had peak discharges of 3,000 to 5,000 ft^3/s (85 to 142 m^3/s) probably was the direct result of increased depths for these flow rates. The velocity of the center of mass of flood waves that had average peak discharges of 10,000 to 20,000 ft^3/s (283 to 566 m^3/s) changed greatly during 1914–70 and reached a maximum average of about 5.7 ft/s (1.74 m/s) in 1914–18 and a minimum average of about 1.8 ft/s (0.55 m/s) in 1964; the velocity for 1914–18 was three times that in 1964, presumably a result of differences in roughness factors.

Major flood waves that occur in the study reach when

the channel is narrow and meanders and when the flood plain is covered by dense vegetation apparently cause a reduction in lag time and an increase in velocity of subsequent major flood waves. Large floodflows exert great force on the channel banks and on objects in the main flow path and enlarge the channel (Burkham, 1972). During a major flood, the main flow path is straight downvalley, and in many places the banks of the meandering stream channel slow the movement of the flood wave. While the meander pattern is intact, part of the flow is directed along the meandering stream channel, and a large amount of turbulence develops along the streambanks, which further slows the movement of water. As a result of the stresses produced by the turbulent forces along the streambanks and around other stationary objects, channel changes eventually take place—banks erode, trees are uprooted and flushed downstream, grass is removed, alluvial fans at the mouths of tributaries are destroyed, and dikes that protect cropland are breached. These changes result in a wider and cleaner stream channel that is more conducive to the rapid movement of major flood waves; for example, the major flood of December 24, 1965, enlarged the channel, and the flood waves of January 2, 1966, and August 13, 1967, moved through the study reach at relatively rapid velocities. The major floods during 1905–17 undoubtedly caused the lag times of the flood waves of October 5, 1914, and July 14, 1919, to be about 14 hours instead of more than 40 hours, the lag time that probably would have occurred if the stream channel and flood plain had remained intact during the 1905–17 floods. The eradication of bottom-land vegetation in a 5.5-mi (8.8-km) length of the study reach may have contributed to the reduced lag time for the August 13, 1967, flood.

TEMPORAL CHANGES IN SPATIAL TRANSFORMATION OF FLOOD WAVES

Two principal types of flood-wave movement, uniformly progressive and reservoir action, have been described in the literature (Carter and Godfrey, 1960, p. 82). Uniformly progressive refers to the downstream movement of a flood wave as a kinematic wave that does not change in shape; uniformly progressive flood wave movement occurs under ideal conditions in a prismatic channel in which the variation in resistance along the channel is small. Reservoir action refers to the transformation of a flood wave caused by reservoir pondage which results when the channel is irregular and the variation in resistance along the channel is large. Both types of flood-wave movement apparently occurred in the study reach during 1914–70.

Temporal changes in the amount of transformation of

a flood wave as the wave moves through the study reach, and the reasons for these changes, are described in the following sections. The effects of channel changes on the results of flood routing using the Muskingum method (Carter and Godfrey, 1960) also are described.

FLOOD HYDROGRAPHS

More than 250 sets of inflow and outflow hydrographs for 1914–70 were used to study the temporal changes in flood wave transformation in the study reach; however, for purposes of this report, hydrographs for four periods—July 14–16, 1919, September 3–5, 1925, July 23–25, 1955, and January 11–17, 1960—were selected to illustrate the changes (figs. 8, 9, and 10). A brief description of the flow in the study reach immediately prior to the four flood events is given as background for later discussions of the factors that cause temporal changes in flood wave attenuation.

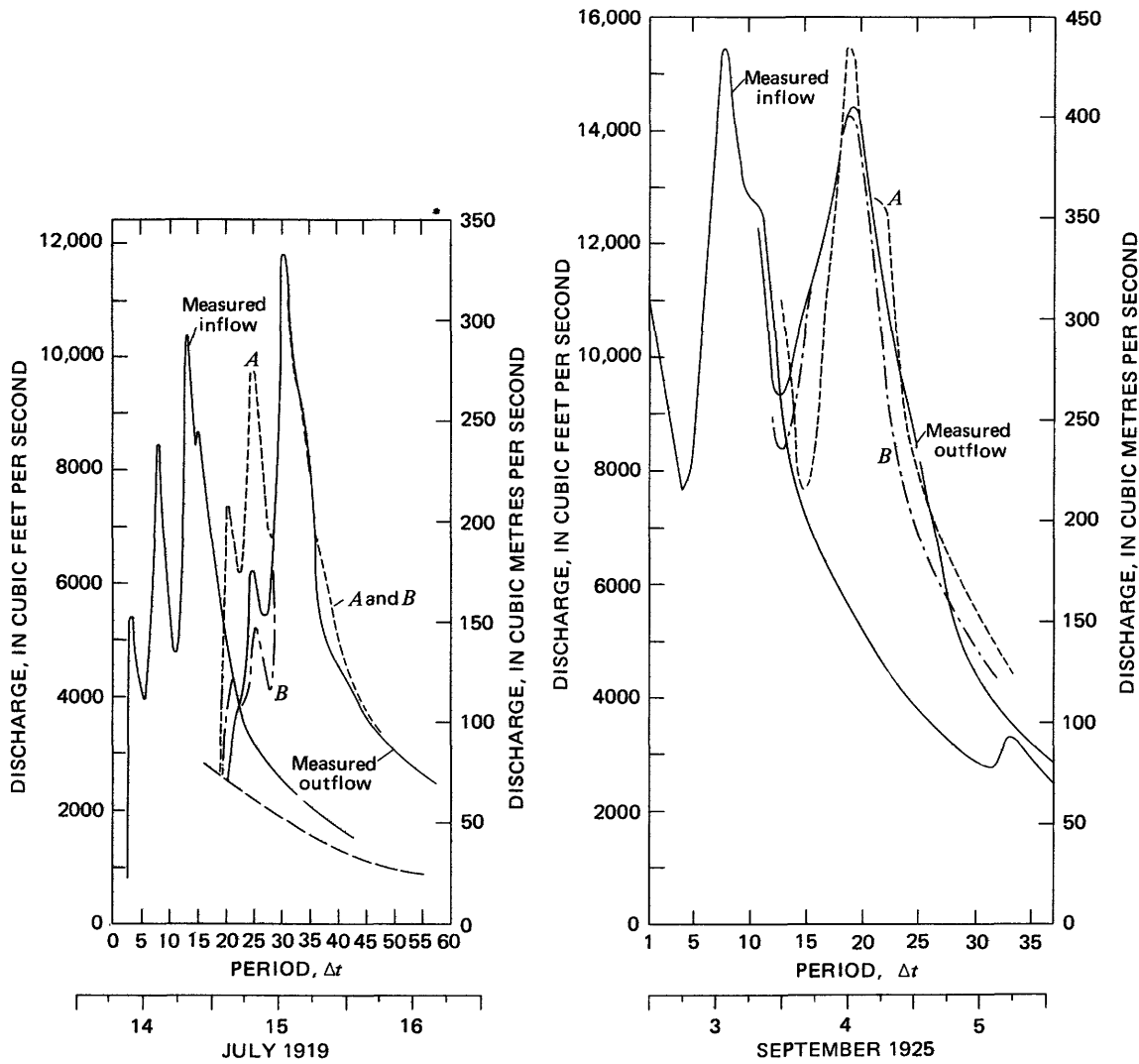
The flood of July 14–16, 1919, which consisted of three waves (fig. 8), was the first large flood in more than a year, although the daily inflow at the upstream end of the study reach ranged from 250 to 950 ft³/s (7.1 to 27 m³/s) for 2 months prior to July 14. The sharp peaks of the inflow waves are typical of flash floods—floods that have large peak rates and small volumes—produced by thunderstorms. The sharp peaks of the outflow waves are typical of those during 1914–27.

Several floods immediately preceded the flood of September 3–5, 1925 (fig. 8). A flood that had a peak discharge of about 10,000 ft³/s (283 m³/s) passed through the study reach during July 31–August 1, and about 20 floods that had smaller peaks followed between August 2 and September 3. The flood of September 3–5 probably was the result of local thunderstorm activity during a large convergence storm or large frontal storm.

The first flood in the summer of 1955 occurred July 11–12 and had a peak discharge of about 5,000 ft³/s (142 m³/s). Prior to July 11, the flow was less than 50 ft³/s (1.4 m³/s), and after about July 15, the flow was less than 200 ft³/s (5.7 m³/s) until the arrival of the thunderstorm that produced the flood of July 23–25; this flood consisted of two waves (fig. 9).

The flood of January 11–17, 1960, which was the result of rainfall and snowmelt, had the highest peak rate of any flood since 1952 (fig. 10). A flood that had a peak discharge of about 5,000 ft³/s (142 m³/s), however, occurred on December 27–29, 1959. The flow prior to December 27 was about 20 ft³/s (0.6 m³/s), and the flow after December 29 was less than 500 ft³/s (14 m³/s).

Flood waves during 1914–27 generally retained their inflow shape (shape at the upstream end of study reach) as they moved through the study reach (fig. 8), and the flood-wave movement approximated a uniformly progressive one; however, the uniformly progressive



EXPLANATION

----- A -----
 The flood of July 1919 was routed assuming continuity of flow. Factors used in the routing are Δt , time units of computation or routing periods; K , slope of the storage-weighted discharge relation in which storage = $K[xI + (1-x)O]$; x , a dimensionless constant that weights the inflow, I , and the outflow, O , in the storage-weighted discharge relation; y , number of subreaches of traveltime used in the routing; and N , number of complete cycles of routing used in synthesizing the outflow hydrograph
 $\Delta t = 1$ hour = 1 period
 $K = 17$ hours
 $x = 0.5$
 $y = 17$ subreaches of traveltime
 $N = 17$ cycles of routing

----- B -----
 The flood was routed assuming that infiltration occurred only during the first two waves, and the flow at the beginning of each of the 17 cycles of routing was depleted according to the equation in which
 $q_f = 0.058I_b$
 q_f = infiltration rate, in cubic feet per second, and
 I_b = inflow at the beginning of the cycle, in cubic feet per second

Other factors used in the routing are as described for curve A
 Estimated inflow from tributaries along the study reach

The flood of September 1925 was routed assuming continuity of flow. Factors used in the routing are Δt , time units of computation or routing periods; K , slope of the storage-weighted discharge relation in which storage = $K[xI + (1-x)O]$; K_o , slope of the storage-weighted discharge relation for the part of the flood that is not contained in the stream channel—the overbank component of the flood; K_w , slope of the storage-weighted discharge relation for the part of the flood that is contained in the stream channel—the within-bank component of the flood; x , a dimensionless constant that weights the inflow, I , and the outflow, O , in the storage-weighted discharge relation; y , number of subreaches of traveltime used in the routing; y_o , number of subreaches of traveltime used in routing of the overbank component of the flood; y_w , number of subreaches of traveltime used in routing of the within-bank component of the flood; and N , number of complete cycles of routing used in synthesizing the outflow hydrograph

----- A -----	----- B -----
$\Delta t = 2$ hours = 1 period	$\Delta t = 2$ hours = 1 period
$K = 22$ hours	$K_o = 22$ hours
$x = 0.5$	$K_w = 18$ hours
$y = 11$ subreaches of traveltime	$x = 0.45$
$N = 11$ cycles of routing	$y_o = 11$ subreaches of traveltime
	$y_w = 9$ subreaches of traveltime
	$N = 1$ cycle of routing

FIGURE 8.—Measured and synthesized floodflow, July 14–16, 1919, and September 3–5, 1925. The inflow was measured at the Gila River at head of Safford Valley, near Solomon gaging station, and the outflow was measured at the Gila River at or near San Carlos gaging station. The synthesized outflow was obtained using the inflow hydrograph and the standard Muskingum flood-routing method (Carter and Godfrey, 1960) or the Muskingum method as modified in this report.

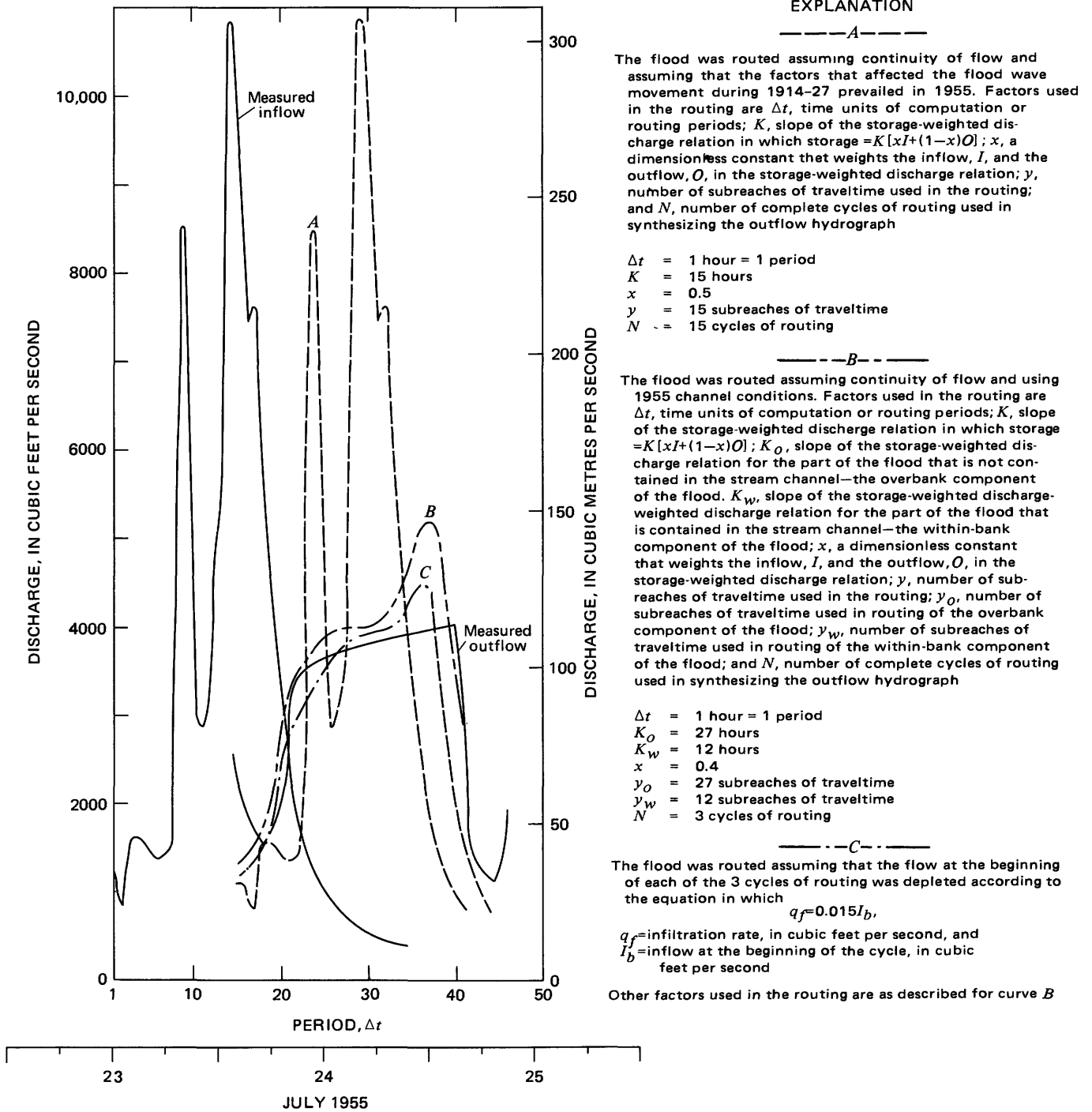


FIGURE 9.—Measured and synthesized floodflow, July 23–25, 1955. The inflow was measured at the Gila River at head of Safford Valley, near Solomon gaging station, and the outflow was measured at the Gila River at Calva gaging station. The synthesized outflow was obtained using the inflow hydrograph and the standard Muskingum flood-routing method (Carter and Godfrey, 1960) or the Muskingum method as modified in this report.

flood-wave movement only applies to floods that were not reduced greatly by infiltration. Infiltration during many floods in the 1914–27 period significantly reduced the size of the floods, and in many instances the inflow shapes were altered.

From about 1935 to 1970, floods were transformed

greatly as they moved through the study reach, probably as a result of reservoir action (figs. 9, 10). Infiltration also may have been a cause for the change in inflow shape.

Significant temporal changes in the attenuation of peak rates moving through the study reach apparently

EXPLANATION

—A—

The July 1919 flood was routed assuming continuity of flow and assuming that the factors that affected the flood wave movement during 1914-27 prevailed in 1960. Factors used in the routing are Δt , time units of computation or routing periods; K , slope of the storage-weighted discharge relation in which storage = $K[xI+(1-x)O]$; x , a dimensionless constant that weights the inflow, I , and the outflow, O , in the storage-weighted discharge relation; y , number of subreaches of traveltime used in the routing; end N , number of complete cycles of routing used in synthesizing the outflow hydrograph

- $\Delta t = 2$ hours = 1 period
- $K = 14$ hours
- $x = 0.5$
- $y = 7$ subreaches of traveltime
- $N = 7$ cycles of routing

—B—

The flood was routed assuming continuity of flow and using 1960 channel conditions. Factors used in the routing are Δt , time units of computation or routing periods; K , slope of the storage-weighted discharge relation in which $=K[xI+(1-x)O]$; K_o , slope of the storage-weighted discharge relation for the part of the flood that is not contained in the stream channel—the overbank component of the flood; K_w , slope of the storage-weighted discharge relation for the part of the flood that is contained in the stream channel—the within-bank component of the flood; x , a dimensionless constant that weights the inflow, I , and the outflow, O , in the storage-weighted discharge relation; y , number of subreaches of traveltime used in the routing; y_o , number of subreaches of traveltime used in routing of the overbank component of the flood; y_w , number of subreaches of traveltime used in routing of the within-bank component of the flood; and N , number of complete cycles of routing used in synthesizing the outflow hydrograph

- $\Delta t = 2$ hours = 1 period
- $K_o = 60$ hours
- $K_w = 12$ hours
- $x = 0.4$
- $y_o = 30$ subreaches of traveltime
- $y_w = 6$ subreaches of traveltime
- $N = 6$ cycles of routing

—C—

The flood was routed assuming that the flow at the beginning of each of the 6 cycles of routing was depleted according to the equation in which

$$q_f = 0.015I_b$$

q_f =infiltration rate, in cubic feet per second, and I_b =inflow at the beginning of the cycle, in cubic feet per second

Other factors used in the routing are as described for curve B

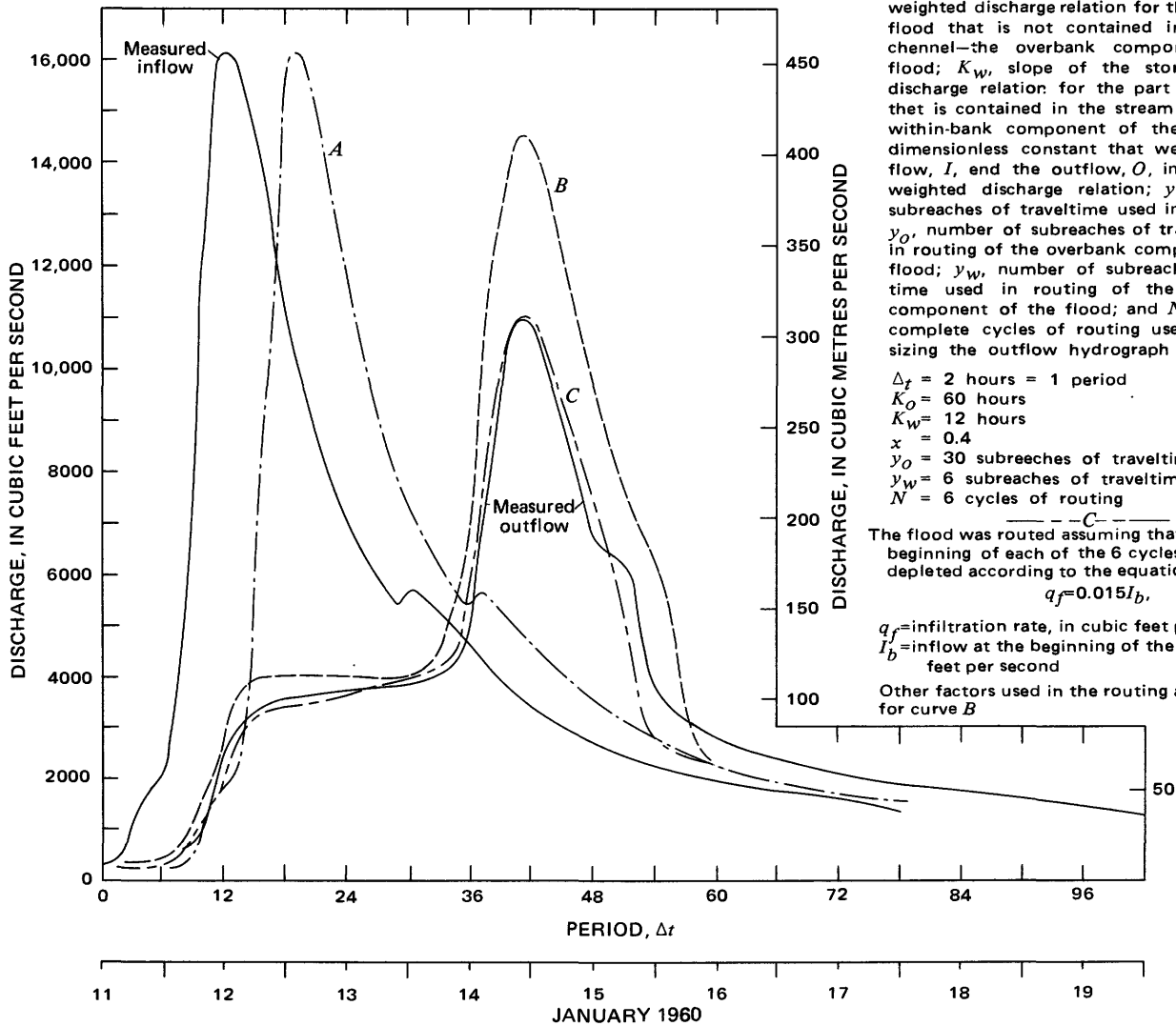


FIGURE 10.—Measured and synthesized floodflow, January 11-19, 1960. The inflow was measured at the Gila River at head of Safford Valley, near Solomon gaging station, and the outflow was measured at the Gila River at Calva gaging station. The synthesized outflow was obtained using the inflow hydrograph and the standard Muskingum flood-routing method (Carter and Godfrey, 1960) or the Muskingum method as modified in this report.

accompanied changes in wave shape (fig. 11). The curves in figure 11 showing the magnitude of temporal change in the attenuation of peak rates were developed using data for floods for which peak discharges at the ends of the study reach were known (Patterson and Somers, 1966). Only data for floods that occurred in 1914-27,

1930-32, and 1944-65 and that had peak discharges at the upstream end of the study reach ranging from 5,000 to 43,000 ft³/s (142 to 1,220 m³/s) were used in the analysis. During 1914-27 and 1930-32, the Gila River was relatively wide, straight, free of bottom-land vegetation and free of alluvial fans. During 1944-65, the

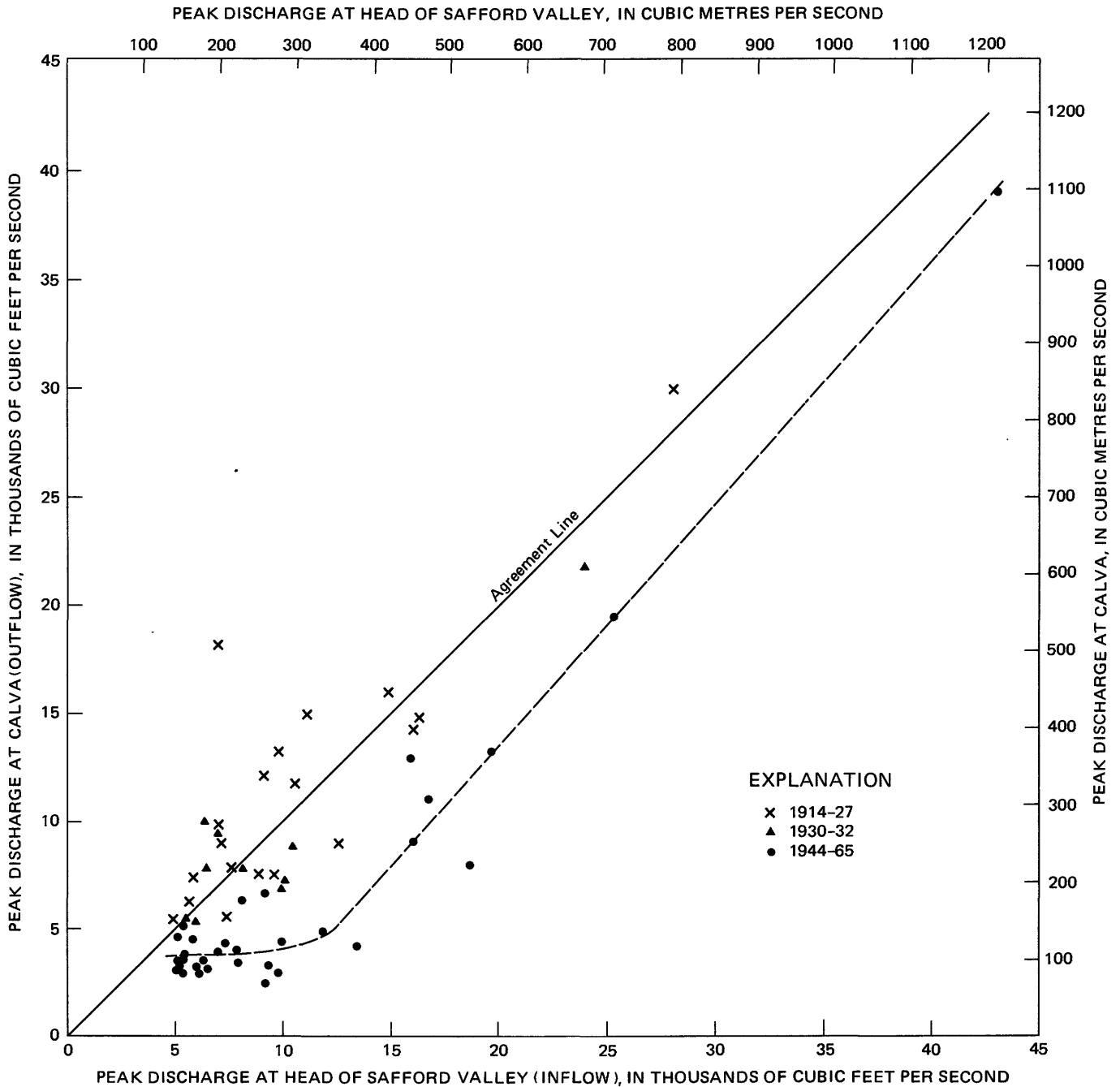


FIGURE 11.—Relation between inflow and outflow for peak discharges of floods moving through the study reach during 1914-27, 1930-32, and 1944-65. The data points are for flood waves that inflow peak discharges ranging from 5,000 to 43,000 ft³/s (142 to 1,220 m³/s). The inflow was measured at the Gila River at head of Safford Valley, near Solomon gaging station, and the outflow was measured at the Gila River at or near San Carlos gaging stations during 1914-27 and at the Gila River at Calva gaging station during 1930-32 and 1944-65. The study reach was 71 miles (114 km) long during 1914-27 and 55 miles (88 km) long during 1930-32 and 1944-65.

stream channel was relatively narrow and had a meandering pattern; the flood plain was densely vegetated and there were alluvial fans on the flood plain at the mouth of tributary streams. The stream channel and flood plain was relatively stable in 1944–65 except in times of rare floods. The study reach was 71 mi (114 km) long during 1914–27 and 55 mi (88 km) long during 1930–32 and 1944–65. During 1914–70, only four floods occurred that had inflow peak rates of more than 43,000 ft³/s (1,220 m³/s); these floods occurred in 1914–16 (fig. 5). The outflow peak rates for floods during 1914–27 and 1930–32 apparently were not significantly smaller than the peak rates of inflow. Peak rates of less than about 13,000 ft³/s (368 m³/s) were reduced to bankfull discharges between 3,000 and 5,000 ft³/s (85 to 142 m³/s) for most floods that occurred in 1944–65, and the average reduction in peak rates ranged from about 7,000 ft³/s (198 m³/s) for floods having inflow peaks of 14,000 ft³/s (396 m³/s) to about 4,000 ft³/s (113 m³/s) for floods having inflow peaks of 44,000 ft³/s (1,250 m³/s) during the same period. The increase in attenuation of peak flow from 1914–27 to 1944–65 probably resulted from temporal increases in reservoir action and infiltration. Decreases in the amount of streamflow contributed by tributary watersheds along the study reach may also have caused some difference in peak outflow. Tributary streamflow ponded behind natural levees during 1944–65 (Burkham, 1972); the natural levees were not present during 1914–27.

MUSKINGUM FLOOD-ROUTING METHOD

The Muskingum flood-routing method was used in the determination of the effects of channel changes on floods because of its simplicity. The variable conditions in the study reach, however, did not agree with the conditions for which the method was developed. Innovations in the Muskingum flood-routing method were made to determine if the method could be altered to fit the variable conditions in the study reach; the innovations also give an indication of the validity of conclusions reached concerning the effects of channel changes on the timing and magnitude of floods. The basic concepts of the Muskingum method given in the following section are from a report by Carter and Godfrey (1960), and the innovations in the method are described in the section "Special Methods." The term "standard Muskingum method" refers to the Muskingum method without innovations, and the term "modified Muskingum method" refers to the Muskingum method with innovations.

BASIC CONCEPTS

The Muskingum method is based on storage generated in a reach during an increment of time and on the

law of continuity of mass. In equation form the law of continuity becomes

$$\bar{O} = \bar{I} - \frac{\Delta S}{\Delta t}, \quad (4)$$

in which

\bar{O} = mean outflow during routing period;

\bar{I} = mean inflow during routing period;

ΔS = net change in storage during routing period; and

Δt = time unit of computation or routing period.

An expanded version of equation (4) is

$$\frac{\Delta t(O_1 + O_2)}{2} = \frac{\Delta t(I_1 + I_2)}{2} - (S_2 - S_1), \quad (5)$$

where O , I , S , and Δt are as previously defined and the subscripts identify the beginning and ending of routing period Δt . The assumption that mean discharge is equal to the simple arithmetic average of the flows at the end points of the interval can be justified if the period is equal to, or less than, the time of travel through the reach and no abrupt changes in flow occur during the routing period (Carter and Godfrey, 1960, p. 85).

In the Muskingum method storage is expressed as a function of the weighted mean flow through the reach as follows:

$$\text{Storage} = K[xI + (1-x)O], \quad (6)$$

in which

I = inflow rate at a given time;

O = outflow rate at a given time;

K = slope of storage-weighted discharge relation that has the dimension of time; and

x = a dimensionless constant that weights the inflow and outflow.

The Muskingum method of expressing storage assumes that the storage varies linearly between the upstream and downstream ends of the reach, that the stage and discharge are uniquely defined at these two places, and that K and x are sensibly constant throughout the range in stage experienced by the flood wave (Carter and Godfrey, 1960, p. 93).

Factor x.—The factor x (equation 6) is chosen so that the indicated volume of storage is the same whether the stage is rising or falling. For spillway discharges from a reservoir, x may be shown to be zero because the reservoir stage and hence the storage are uniquely defined by the outflow; therefore, the rate of inflow has a negligible influence on the storage in the reservoir at any time. For uniformly progressive flow, x equals 0.50, and the inflow and the outflow are equal in weight. In this wave, no change in shape takes place, and the peak discharge remains unaffected. Thus, the value of x will range from 0 to 0.50, with a value of 0.25 as average for river

reaches. No way is known for determining the value of x from the hydraulic characteristics of a channel system in the absence of discharge records.

Factor K.—The factor K has the dimension of time and is the slope of the storage-weighted discharge relation. Generally, the value of K can be determined with much greater ease and certainty than that of x . Equations (5) and (6) may be combined into

$$K = \frac{\Delta t \left(\frac{I_2 + I_1}{2} - \frac{O_2 + O_1}{2} \right)}{x(I_2 - I_1) + (1-x)(O_2 - O_1)} \quad (7)$$

or

$$O_2 = -\frac{(Kx - 0.5\Delta t)}{(K - Kx + 0.5\Delta t)} I_2 + \frac{(Kx + 0.5\Delta t)}{(K - Kx + 0.5\Delta t)} I_1 + \frac{(K - Kx - 0.5\Delta t)}{(K - Kx + 0.5\Delta t)} O_1 \quad (8)$$

or simplified as

$$O_2 = C_0 I_2 + C_1 I_1 + C_2 O_1, \quad (9)$$

where Δt has the same meaning as in equation (4), x and K have the same meaning as in equation (6), and

- I_1, I_2 = total instantaneous inflow to a reach at the beginning of successive times 1 and 2;
 O_1, O_2 = instantaneous outflow at the beginning of successive times 1 and 2; and
 $C_0, C_1,$
 and C_2 represent the fractions in equation (8).

The numerator in equation (7) is the storage increment, which is equal to the inflow minus the outflow, whereas the denominator is the corresponding weighted-flow increment. Equation (8) gives O_2 in terms of three routing coefficients and three known discharges: $I_1, I_2,$ and O_1 . The routing coefficients may be computed from known values of x and K . Equation (9) reduces the routing procedure by the Muskingum method to tabular multiplication and addition. The time increment Δt between successive values of inflow or outflow should be less than $2Kx$ to avoid negative values of C_0 . For many flood-routing problems, the factor K may be assumed to be constant.

SPECIAL METHODS

Significant infiltration occurred during most flow events analyzed in this study, and the factor K was variable, which caused problems in using the Muskingum flood-routing method because the method assumes a continuity of mass and a constant K . The factor K is about equal to the lag time of the center of mass of a

definable part of a flood (Carter and Godfrey, 1960, p. 93), which varies with discharge and time in the study reach (fig. 2). The standard Muskingum flood-routing method gave satisfactory results for floods that had no significant losses of flow and that occurred when the stream channel was wide and relatively free of vegetation. After a narrow stream channel and a densely vegetated flood plain developed, however, the flow in the stream channel during a flood event moved much faster than the flow on the flood plain (fig. 3). Thus, in an attempt to duplicate outflow hydrographs, two values of K were used in the routing.

The inflow hydrographs for floods that occurred after the development of the narrow stream channel were divided at the bankfull discharge into two components—overbank and within bank—before the hydrographs were used in the routing computation. A value for the K factor was assigned to each of the two flow components. The value of K for the overbank component was taken as the lag time of the peak discharge, and K for the within-channel component was assumed to be equal to the lag time of the front of the wave for the within-channel flow.

Using equation (9), each component of the hydrograph was routed through y number of subreaches of traveltime, $K_s = \Delta t$, such that yK_s is equal to the value of K for each component (Carter and Godfrey, 1960). The increment of routing time, Δt , between successive rates of flow was chosen so that the inflow and outflow hydrographs would be defined adequately.

The two flood components were united at the end of a routing cycle and then separated again into overbank and within-bank components; this was done to allow for interchange of water between the two components. The correct timing was assured when the components were reunited by use of the relation

$$\Delta t = K_s = \frac{K_o}{y_o} = \frac{K_w}{y_w}, \quad (10)$$

where $\Delta t, K,$ and y are as previously defined and where the subscripts o and w represent the overbank and within-bank components. Equation (10) then becomes

$$\frac{y_o}{y_w} = \frac{K_o}{K_w}. \quad (11)$$

Equations (10) and (11) show that K_o/K_w subreaches of traveltime for the overbank component correspond to one subreach of traveltime for the within-bank component. The ratio of K_o to K_w must be constant, and both K_o and K_w must be whole numbers in order for the routing to be physically possible; the two flood-wave components are reunited, and a routing cycle is thus com-

pleted each time these two constraints are met. For example, assuming a K_o of 27 and a K_w of 12 for a flood wave, the constant ratio K_o/K_w would be 27/12; 27 and 12 are divisible by 3, therefore, there would be three cycles of routing. In the example four subreaches of traveltime for the within-channel component correspond in time to nine subreaches of traveltime for the overbank component.

Depletion of flood volumes was assumed to be entirely by infiltration. Infiltration was assumed to have occurred during the rising and receding parts of a wave until some critical discharge was reached, as when the forces that restricted the infiltration were equal to the forces that caused the infiltration. The critical discharge probably was different for each flood, and there is no known method to determine its value precisely. For lack of a better method, the estimates of critical discharge were based primarily on comparisons of inflow and outflow hydrographs, as discussed further in the section "Routing of Floods." After critical discharge was reached, some flow from bank storage returned to the stream; no effort was made in the routings to account for the return flow.

The infiltration rate during a cycle of routing time was assumed, as an approximation, to be defined by the relation

$$q_f = AI_b, \quad (12)$$

in which

q_f = infiltration rate for a routing cycle;
 I_b = flow during routing period Δt at the beginning of a routing cycle; and

$$A = \left(\frac{V_I - V_o}{N} \right) \div \left(\frac{V_I + V_o}{2} \right) = \left(\frac{2(V_I - V_o)}{N(V_I + V_o)} \right),$$

in which

V_I = volume of inflow to the study reach from the beginning of a flood wave until the critical inflow discharge is reached;

V_o = volume of floodflow leaving the study reach from the beginning of a flood wave until the critical outflow discharge is reached; and

N = number of complete routing cycles.

The inflow I_b was reduced by the quantity q_f at the beginning of each cycle of routing. The method of estimating critical discharge was different for each routed flood; the methods used are described below.

ROUTING OF FLOODS

FLOODS OF JULY 14-16, 1919, AND SEPTEMBER 3-5, 1925

The last flood wave of the July 1919 flood and the

wave of September 1925 moved through the 71-mi (114-km) reach of the Gila River from the head of Safford Valley to the San Carlos gaging station without large changes in peak discharge and flow distribution with time (fig. 8). The rates of the first two waves of the July 1919 flood, however, were greatly reduced by infiltration.

The standard Muskingum method with $x=0.5$ was used in routing A (fig. 8) for the July 1919 and September 1925 floods. The time increment, Δt , necessary to define the hydrograph was 1 hour for the July 1919 flood and 2 hours for the September 1925 flood. In each routing A, the two floods were assumed to be contained in a wide stream channel. A value of K of 17 hours was used for the July 1919 flood, and 22 hours for the September 1925 flood. The values of K were taken as the lag time of the peak discharges. Tributary inflow contributed to the July 1919 flood, and the estimated rates of tributary inflow are shown in figure 8. The estimated inflow from tributaries was added to the routed flow before the combined routed and tributary flows were plotted.

Routing B for the July 1919 flood was made using the same procedure used in routing A, except that a correction was made for depletion of surface flow by infiltration (fig. 8). Apparently, the first two waves of the flood were almost depleted by infiltration as the flood moved through the study reach, and only minor flow depletion occurred during the third wave; these factors were considered when depletion-of-flow corrections were made and the critical discharge was assumed to have occurred at the end of the second wave. The volume V_I in equation (12) was computed using the relation

$$V_I = \sum_{i=2}^{12} I_i \Delta t, \quad (13)$$

and the volume V_o was computed using the relation

$$V_o = \sum_{i=19}^{29} O_i \Delta t - \sum_{i=19}^{29} (I_i)_i \Delta t, \quad (14)$$

where the subscript i represents the number of routing periods and I_i represents tributary inflow; 2 and 19 in equations (13) and (14), respectively, refer to the periods in which the flood arrived at the two measuring sites. At period 29 during the outflow, the estimated critical discharge was reached; the 12th period is about the time when the inflow corresponding to the critical outflow discharge occurred. The computed values of V_I

and V_o are 52,000 and 17,600 ft³/s-periods (1,470 and 498 m³/s-periods), respectively. Using these values in equation (12),

$$q_f = 0.058I_b \quad (15)$$

The inflow I_b at the beginning of each of the 17 cycles of routing was reduced by the quantity q_f before the routing was made. The infiltration correction for the first cycle of routing was applied to the inflows starting at period 2 and ending at period 12 (fig. 8). The beginning and ending points in applying infiltration corrections for the other cycles were lagged by the number of periods in a cycle. The correction for the last cycle of routing was applied to inflows starting at period 18 and ending at period 28.

The outflow synthesized for the September 1925 flood by routing *A* did not agree closely with the measured outflow; however, the timing of the peak discharge was satisfactory (fig. 8). Other routings of the September 1925 flood were made using different values of x in the standard Muskingum method; the results of these routings did not indicate a significant improvement over routing *A* and are not shown in figure 8.

Routing *B* of the September 1925 flood was made using an x of 0.45, a K_o of 22 hours (11 routing periods), and a K_w of 18 hours (fig. 8). The depletion of flow by infiltration apparently was minor, and no corrections were applied. The bankfull discharge for the flood probably was 8,000 to 12,000 ft³/s (227 to 340 m³/s) (fig. 2); bankfull discharge was estimated to be 12,000 ft³/s (340 m³/s), and the hydrograph was separated into components at that rate.

FLOOD OF JULY 23-25, 1955

Routing *A* of the flood hydrograph was made using a value of K of 15 hours and a value of x of 0.5 in the standard Muskingum method (fig. 9). Routing *A* gives an approximate indication of what the timing and shape of the outflow hydrograph would be if the flood had occurred when there was no flood plain and the stream channel was wide and relatively straight. The K of 15 hours was taken from the trend line in figure 2A for an average peak discharge of 11,000 ft³/s (312 m³/s), which is the peak rate of flow at the inflow site. An x of 0.5 was selected so there would be no change in the shape of the hydrograph and no attenuation of the flow rates as a result of reservoir action.

Other routings of the July 1955 flood were made using different values of K and x in the standard Muskingum method; however, the timing, peak rate, and distribution of synthesized outflow for these routings did not match those of measured outflow satisfactorily, and the results are not shown in figure 9.

Routing *B* was made using two values of K and different values of x in the modified Muskingum method (fig. 9). For routing *B*, inflow was divided into overbank and within-bank components using 4,000 ft³/s (113 m³/s) as bankfull discharge. The time increment Δt necessary to define the inflow and outflow hydrographs was 1 hour. The value of K_o , which was taken as the lag time of the peak discharge, was 27 hours. The value of K_w was assumed to be about equal to the difference in time from the occurrence of 2,000 ft³/s (57 m³/s) on the rising limb of the inflow hydrograph to the occurrence of 2,000 ft³/s on the rising limb of the outflow hydrograph; the difference was 12 hours. The two flood wave components were reunited at the ends of four subreaches of traveltime for the within-bank component, which resulted in three cycles of routing. The synthesized outflow was obtained using an x of 0.4 for both components (fig. 9, curve *B*). No allowance was made for depletion of streamflow in the routing; therefore, the synthesized outflow is larger than measured outflow.

Routing *C* was made using the same procedure used in routing *B*, except that a correction was made for loss of surface flow (fig. 9). The flow depletion is assumed to have resulted entirely by infiltration, and equation (12) was used in the infiltration computation. The volume V_I was computed using the relation

$$V_I = \sum_{i=6}^{31} I_i \Delta t, \quad (16)$$

and the volume V_o was computed using the relation

$$V_o = \sum_{i=18}^{43} O_i \Delta t. \quad (17)$$

The flood arrived at the two measuring sites at periods 6 and 18, respectively. The recession of outflow reached the estimated critical discharge of 1,200 ft³/s (34 m³/s) at period 43; a value of 12, representing lag time, was subtracted from 43 to estimate the period when the inflow corresponding to the critical outflow discharge occurred. The computed values of V_I and V_o are 97,400 and 80,120 ft³/s-periods (2,760 and 2,270 m³/s-periods), respectively. Using these values in equation (12),

$$q_f = 0.015I_b \quad (18)$$

The inflow I_b at the beginning of each of the three cycles of routing was reduced by the quantity q_f before the routing was made. The infiltration correction for the first cycle of routing was applied to the inflows starting

at period 6 and ending at period 31 (fig. 9). The beginning and ending points in applying infiltration corrections for the other cycles were lagged by the number of periods in a cycle. The correction for the last cycle of routing was applied to inflows starting at period 14 and ending at period 39.

FLOOD OF JANUARY 11-17, 1960

Routing *A* of the flood hydrograph was made using a value of K of 14 hours and a value of x of 0.5 in the standard Muskingum method (fig. 10). The time increment Δt necessary to define the inflow and outflow hydrographs was 2 hours. The K of 14 hours was taken from the trend line in figure 2A for an average peak discharge of 16,000 ft³/s (453 m³/s), which is the peak rate of flow at the inflow site. Routing *A* gives an approximate indication of what the timing and shape of the outflow hydrograph would have been if the flood had occurred when there was no flood plain and the stream channel was wide and relatively straight.

For routing *B* the inflow wave was divided into over-bank and within-bank components using 4,000 ft³/s (113 m³/s) as bankfull discharge (fig. 10). The value of K_o was taken as 60 hours or 30 routing periods, and the value of K_w was taken as 12 hours or 6 periods. Six routing cycles were used in the analysis.

Routing *B* for the January 1960 flood was made using the factors described above and different values of x in the modified Muskingum method (fig. 10). The synthesized outflow was obtained using an x value of 0.4, and the hydrograph compares favorably in shape and timing with the hydrograph of measured outflow; however, the synthesized outflow is larger than measured outflow because no allowance was made for infiltration.

A correction was made for loss of surface flow in routing *C* of the flood wave (fig. 10). During the January 1960 flood there were no diversions of flow for irrigation use (U.S. Geological Survey, 1961); therefore, the flow depletion is assumed to have resulted entirely from infiltration, and equation (12) was used in the infiltration computation. The volume V_I was computed using the relation

$$V_I = \sum_{i=2}^{48} I_i \Delta t, \quad (19)$$

and the volume V_o was computed using the relation

$$V_o = \sum_{i=8}^{54} O_i \Delta t. \quad (20)$$

The recession of outflow reached the estimated critical discharge of 4,000 ft³/s (113 m³/s) at period 8; a value of 6 representing lag time, in periods, was subtracted from 8 to estimate the period when inflow corresponding to the critical outflow discharge occurred. The numbers 2, 8, 48, and 54 refer to routing periods, which are shown in figure 10. The values of V_I and V_o are 311,500 and 239,800 ft³/s-periods (8,820 and 6,790 m³/s-periods), respectively. Using these values in equation (12),

$$q_f = 0.045 I_b. \quad (21)$$

The inflow I_b at the beginning of each of the six cycles of routing was reduced by the quantity q_f before the routing was made. The infiltration correction for the first cycle of routing was applied to the inflows starting at period 2 and ending at period 48 (fig. 10). The beginning and ending points in applying infiltration corrections for the other cycles were lagged by the number of periods in a cycle. The correction for the last cycle of routing was applied to inflows starting at period 6 and ending at period 52.

The critical discharge—the discharge at which the infiltration became zero—apparently is larger than the assumed discharge because the synthesized outflow is less than 3,000 ft³/s (85 m³/s) when the measured outflow was 4,000 ft³/s (113 m³/s). If the critical discharge is larger than the assumed discharge, the volume of infiltration ($V_I - V_o$) probably is larger than the computed infiltration. The match of hydrographs of measured and synthesized flows is good throughout most of the flood, and the match is assumed to be satisfactory for this study.

DISCUSSION OF RESULTS

The lack of change in inflow shapes of flood waves during 1914-27 indicates little or no reservoir action. Small translatory waves may have helped the flood waves retain their inflow shape during 1914-27. A rapid rise of a flood wave in an unvegetated ephemeral stream often takes place through a succession of small surges (Leopold and Miller, 1956, p. 4); an increase in stage occurs when a surge overrides an earlier surge as the flow progresses downstream. The result is a mechanism shortening the rise time, which seems to be independent of channel storage (Renard and Keppel, 1966, p. 47) and reservoir action.

Large quantities of water infiltrated the sides and bottom of the channel during most flow events during 1914-27; however, the effects of the flow depletion due to infiltration on the transformation of flood waves are not known. A reduction in flow volume may cause a change in the shape of a flood wave as it passes through a reach. Infiltration of water into a dry channel that is not sealed by silt and clay generally takes place rapidly

on the arrival of a flood wave. Under these channel conditions, which may have prevailed during 1914–27, a large part of the infiltration losses may have occurred on the rising limb of the flood wave, which would cause a decrease in the rise time (Renard and Keppel, 1966, p. 39) and an increase in the sharpness of the flood wave—a situation in opposition to the rounding effect caused by reservoir action. The author found, however, in channels sealed by silt and clay and having moving boundaries, the largest part of the infiltration losses generally occurred during the recession limb of the flood wave (Burkham, 1970b, 1970c). The silt and clay is set in motion during high streamflow velocities, and large quantities of water infiltrate when the silt and clay seal is removed. Large amounts of infiltration during recession have a tendency to increase the slope or sharpness of the recession part of the flood.

The last outflow wave of the July 1919 flood was similar in shape and magnitude to the third inflow wave, and the synthesized flow for the third wave—assuming a continuity of flow and an x value of 0.5—agrees very well with the measured flow (fig. 8). The synthesized outflow for the first two waves, however, was much larger than the measured outflow. The synthesized outflow—after a correction for infiltration was made (fig. 8, curve *B*) using equation (12)—resulted in the peak rate for the first wave being too large and the peak rate for the second wave being too small. Undoubtedly the infiltration for a given inflow rate was larger for the first wave than for the second or third wave.

Considering all the factors previously discussed and those discussed in the section "Flood Hydrographs," the author concludes that during the July 1919 flood (1) a large part of the channel was dry and was not sealed with a layer of fine sediment, and the void space available to store infiltrated water was relatively small when the flood arrived; (2) the infiltration rate for a given inflow rate was relatively large during the first wave but probably was about zero during the third wave; (3) there was little if any return flow to the channel from bank storage after the flow passed through the study reach; and (4) using the standard Muskingum method, the synthesized outflow for the third wave agrees closely with measured outflow—however, the inflow and a close approximate value of K were known.

The synthesized flow for the recession part of the September 1925 flood, assuming a continuity of flow and an x value of 0.5 (fig. 8, curve *A*), agrees well with the measured flow; however, the synthesized flow for the rising part of the flood was smaller and the peak rate was larger than the measured flow (fig. 8). Routing *B* of the flood hydrograph is in closer agreement for the rising limb and peak rate than routing *A*; however, the agreement for the recession limb is not as good. A closer

agreement between synthesized and measured flows probably could have been obtained by additional curve-fitting adjustments in the flood-routing method, but the final product would not contribute significantly to this report.

For the September 1925 flood, the author concludes that (1) infiltration was insignificant; (2) in general the flood wave retained its inflow shape as it moved through the study reach; (3) the reduction in peak discharge was less than 7 percent of the inflow peak, and this reduction is less than the probable error in the flood data; (4) although the size of the channel and bankfull discharge is unknown, a partly developed flood plain probably existed at the time of the flood, and water in the stream channel moved faster than water on the flood plain; and (5) the synthesized outflow obtained using one value of K and an x of 0.5 in the standard Muskingum method agree with measured outflow just as well as the synthesized flows obtained using two values of K and an x of 0.45 in the modified Muskingum methods.

Efforts to synthesize the outflow for the flood of July 1955 by varying x and K in the standard Muskingum method were unsuccessful. When the correct timing and rate for the peak discharge were obtained, the rate and distribution of flow during the rising and receding limbs of the wave were incorrect. Adequate duplication of the rapidly decreasing flow, which occurred after the peak discharge, could only be achieved by using an x value of 0.5 in the routing, but then the rate and flow distribution for the rest of the wave were incorrect.

The shape and timing of the synthesized outflow for the flood of July 1955 obtained in routing *B* agrees fairly well with the measured outflow; therefore, the author assumes that the innovation of the use of two values of K in the routing of the 1955 flood was justified (fig. 9, curve *B*). The infiltration function (eq. 18) used in making the loss-of-flow correction in routing *C* apparently does not adequately describe the true streamflow-to-infiltration relation because there is a significant difference in shape and timing between synthesized and measured outflow after the correction is applied.

The attenuation effects of reservoir action and infiltration of the flood of July 1955 reduced the peak discharge to bankfull discharge (fig. 8); the attenuation of the peak was about 60 percent of the inflow peak rate. The attenuation caused by reservoir action cannot be determined precisely for the flood because of the large amount of infiltration. The amount of reduction in peak flow for a wave caused by reservoir action is known to be closely related to the volume of the wave, and therefore the amount of reduction is closely related to the amount of infiltration. If curve *B* in figure 9 is assumed to represent the outflow when continuity of flow existed, the attenuation of the peak flow caused by the reservoir

action was about 7,900 ft³/s (223 m³/s), which leads to the assumption that the infiltration in the reach during the flood caused a reduction in peak discharge of 1,200 ft³/s (34 m³/s). Assuming that no attenuation of the peak discharge would have occurred if a flood similar to the July 1955 flood had passed through the reach during 1914–27, the effects of channel changes during 1927–55 on the attenuation of the peak discharge of the July 1955 flood amounted to about 7,900 ft³/s (223 m³/s), or 72 percent of the peak discharge.

The hydrograph of measured outflow for the flood of January 1960 could not be duplicated adequately using the standard Muskingum method. A good agreement between measured and synthesized outflows was obtained when two values of K and a correction for infiltration were used in the modified Muskingum method (fig. 10). A significant rate of flow, presumably from bank storage, returned to the stream channel during the recession of the flood; no correction for return flow from bank storage was made.

The attenuation of the peak discharge for the flood of January 1960 was 5,000 ft³/s (142 m³/s). Assuming that curve B in figure 10 represents the outflow hydrograph if infiltration had not occurred, the amount of attenuation caused by reservoir action would be about 1,500 ft³/s (42 m³/s). The infiltration in the reach during the flood therefore caused a reduction in peak discharge of about 3,500 ft³/s (100 m³/s), difference between the peak discharge shown in curve B and the measured outflow (fig. 10). As previously discussed, the attenuation in peak flow caused by reservoir action is closely related to the attenuation caused by infiltration, and there is no known way of separating the two effects when infiltration occurs. The attenuation caused by reservoir action is probably larger than 1,500 ft³/s (42 m³/s), which makes the attenuation caused by infiltration smaller than 3,500 ft³/s (100 m³/s). The difference between the volumes of the floods of January 1960 and July 1955 probably is the main reason the attenuation of the January 1960 flood was only 30 percent, whereas the attenuation of the July 1955 flood was more than 60 percent. The effects of channel changes during 1914–70 on the reduction of the peak discharge of the flood of January 1960 are assumed to have been more than 1,500 ft³/s (42 m³/s).

SUMMARY AND CONCLUSIONS

The channel changes in the Gila River during 1914–70 caused significant differences in the timing, magnitude, and transformation of flood waves in the 55-mi (88-km) reach of the Gila River in Safford Valley. The channel changes consisted of (1) narrowing of the stream channel from about 2,000 ft (600 m) to less than 300 ft (90 m), (2) development of a flood plain, stream-

channel meander pattern, natural levees along the stream channel, and alluvial fans at the mouths of tributaries, and (3) spreading of dense saltcedar along the flood plain. Except for small flood waves having peak discharges less than about 500 ft³/s (14 m³/s), the timing and velocity of all the waves were affected by the channel changes. For 1914–27, the trend was toward a gradual increase in downstream velocity of the center of mass of flood waves as the peak discharge increased, which is indicative of flow in wide channels where the resistance to water movement is mainly along the bottom. During 1943–70, the trend was toward an increase in downstream velocity as the peak discharge increased from about 500 to about 4,000 ft³/s (14 to 113 m³/s), a decrease in velocity as the peak discharge increased from about 4,000 to 20,000 ft³/s (113 to 566 m³/s), and an increase in velocity for a peak discharge greater than 20,000 ft³/s (566 m³/s) (table 2). Major floods that occurred when the stream channel was fully developed and the flood plain was densely covered with saltcedar partially cleared the channel and caused a reduction in lag time and an increase in velocity of subsequent floods.

The channel changes in the Gila River during 1914–70 caused an increase in the attenuation of flood waves as they moved through the study reach. During 1914–27, when the channel was wide and relatively free of vegetation, flood waves moved through the reach without large changes in inflow shapes; however, significant reductions in peak rates occurred when the infiltration was relatively large. After the stream channel developed and the flood plain became densely vegetated, flow in the stream channel moved at a much higher velocity than flow on the flood plain, which resulted in an elongation of floodwaves and a reduction in peak discharge. For flashy floods (floods that had large inflow peaks and small inflow volumes) the combined attenuation effects of reservoir action and infiltration reduced the peak flow to bankfull discharge—about 4,000 ft³/s (113 m³/s) at the downstream end of the study reach.

The standard Muskingum flood-routing method gave satisfactory results for floods that occurred when the

TABLE 2.—Velocity of the center of mass of flood waves and approximate values of Manning n for selected peak discharges

Period of record used in analysis (water year)	Peak discharge ¹ (ft ³ /s)	Velocity of center of mass of floodwave ² (ft/s)	Approximate n value ³
1914–27	300–500	2.9–3.1	0.02–0.04
1961–70		2.9–3.4	0.02–0.04
1914–27	3,000–5,000	4.2–4.7	0.02–0.04
1961–70		6.0–6.9	0.02–0.04
1914–27	15,000–20,000	5.2–5.7	0.02–0.04
1961–70		1.8–2.3	0.06–0.14

¹Average of peak discharges at the ends of the reach.

²Downstream velocity was determined by dividing the length of main flow path by lag time of the center of mass of flood wave, which was obtained from trend lines in figure 2.

³The Manning velocity equation is $V = 1.49 (R)^{2/3} S^{1/2}$, in which R is hydraulic radius, S is slope of energy gradient, and n is a roughness coefficient.

stream channel was wide and free of vegetation and that had no significant losses of flow; however, the standard Muskingum method was not adequate for the routing of floods that occurred after a narrow stream channel and a densely vegetated flood plain developed. Innovations in the Muskingum flood-routing method were made to fit the variable conditions in the study reach. The hydrographs for floods that occurred after the development of the narrow stream channel were divided into overbank and within-bank components before they were routed. The overbank component consists of flow greater than bankfull discharge, and the within-bank component consists of flows less than bankfull discharge. A factor, K , was assigned to each of the flow components. Using the standard Muskingum equation, each component of the hydrograph was routed through several subreaches of traveltime. Owing to infiltration, adjustments in the flood-routing method were made on the assumption that the infiltration rate was linearly related to the inflow rate for each of the subreaches of traveltime. Infiltration is assumed to have occurred during the rising and recession parts of a wave until the forces that restricted the infiltration were equal to the forces that caused the infiltration. The critical discharge was estimated. The innovation in flood routing was partly successful in that there was fair agreement between hydrographs of measured and synthesized outflows.

The conclusions reached as a result of this study are as follows:

1. The size and meander pattern of the stream channel of the Gila River are determined by past dominant flows. The stream channel is wide and straight at the end of a period in which high flows were dominant and is narrow and has a meander pattern at the end of a period in which low flows were dominant.
2. The stream-channel and flood-plain system, when fully developed for a dominant flow, has a persistent effect on floods. A low-flow system—developed by and for low flows—attenuates flood peaks passing through the reach; the peak flows of flashy floods may be reduced to bankfull discharge. A high-flow system—developed by and for high flows—does not increase flood rates; however, streamflow from side tributaries along the study reach may contribute more significantly to peak rates in the Gila River when a high-flow system is in effect than when a low-flow system is in effect.
3. The downstream velocity of the center of mass of flood waves that had peak discharges of between 10,000 to 20,000 ft³/s (283 to 566 m³/s) during 1914–27 may have been as much as three times that for the same rates during 1943–70.
4. A low-flow system may change rapidly to a high-flow system when a series of major floods occurs; however, several years of low flow are required before a high-flow system changes to a low-flow system; it took about 50 years for the present (1970) low-flow system to develop (Burkham, 1972).
5. Annual peak flows measured at the downstream end of the study reach reflect, among other things, the persistent effect of the upstream system, and therefore they are not random in time. Because of changes in the system, the data of peak flows collected at the downstream end of the study reach during 1914–27 are from a different population than the data of peak flows for the period 1943–70.
6. The stream channel of the Gila River can be widened and straightened in an attempt to duplicate a high-flow system; however, it will be difficult to maintain the artificial channel unless large flows occur. Conversely, it would be difficult to develop and maintain a low-flow system during a period in which large flows are dominant.
7. Widening and straightening the stream channel will increase the conveyance capacity of the Gila River; however, the widening and straightening of the channel may increase flood rates at the downstream end of the valley (See conclusions 2 and 6.)
8. Outflow rates for flood waves moving through the study reach when a high-flow system is in effect can be synthesized using the standard Muskingum method if an inflow hydrograph and an approximate value for Muskingum's K are available. The standard Muskingum method, however, is not suitable for the routing of flood waves—except possibly for extremely small or large waves—that occur when a low-flow system is in effect.

REFERENCES CITED

- Barnes, H. H., Jr., 1967, Roughness characteristics of natural channels: U.S. Geol. Survey Water-Supply Paper 1849, 213 p.
- Bryan, Kirk, 1926, Pedestal rocks formed by differential erosion and channel erosion of the Rio Salado, Socorro County, New Mexico: U.S. Geol. Survey Bull. 790-A, 19 p.
- Burkham, D. E., 1970a, Precipitation, streamflow, and major floods at selected sites in the Gila River drainage basin above Coolidge Dam, Arizona: U.S. Geol. Survey Prof. Paper 655-B, 33 p.
- 1970b, Depletion of streamflow by infiltration in the main channels of the Tucson basin, southeastern Arizona: U.S. Geol. Survey Water-Supply Paper 1939-B, 36 p.
- 1970c, A method for relating infiltration rates to streamflow rates in perched streams, *in* Geological Survey research 1970: U.S. Geol. Survey Prof. Paper 700-D, p. D266-D271.
- 1972, Channel changes of the Gila River in Safford Valley, Arizona, 1846–1970: U.S. Geol. Survey Prof. Paper 655-G, 24 p.

- 1976, Hydraulic effects of changes in bottom-land vegetation on three major floods, Gila River in southeastern Arizona: U.S. Geol. Survey Prof. Paper 655-J, 14 p.
- Burkham, D. E., and Dawdy, D. R., 1970, Error analysis of streamflow data for an alluvial stream: U.S. Geol. Survey Prof. Paper 655-C, 13 p.
- Carter, R. W., and Godfrey, R. G., 1960, Storage and flood routing: U.S. Geol. Survey Water-Supply Paper 1543-B, p. 81-104.
- Culler, R. C., and others, 1970, Objectives, methods, and environment—Gila River Phreatophyte Project, Graham County, Arizona: U.S. Geol. Survey Prof. Paper 655-A, 25 p.
- Dalrymple, Tate, and Benson, M. A., 1967, Measurement of peak discharge by the slope-area method: U.S. Geol. Survey Techniques Water-Resources Inv., book 3, chap. A-2, 12 p.
- Gatewood, J. S., Robinson, T. W., Colby, B. R., Hem, J. D., and Halpenny, L. C., 1950, Use of water by bottom-land vegetation in lower Safford Valley, Arizona: U.S. Geol. Survey Water-Supply Paper 1103, 210 p.
- Leopold, L. B., and Miller, J. P., 1956, Ephemeral streams—Hydraulic factors and their relation to the drainage net: U.S. Geol. Survey Prof. Paper 282-A, 37 p.
- Linsley, R. K., Kohler, M. A., and Paulhus, J. L. H., 1949, Applied Hydrology: New York, McGraw-Hill Book Co., 689 p.
- Olmstead, F. H., 1919, Gila River flood control—A report on flood control of the Gila River in Graham County, Arizona: U.S. 65th Cong., 3d sess., Senate Doc. 436, 94 p.
- Patterson, J. L., and Somers, W. P., 1966, Magnitude and frequency of floods in the United States—Part 9, Colorado River basin: U.S. Geol. Survey Water-Supply Paper 1683, 475 p.
- Renard, K. G., and Keppel, R. V., 1966, Hydrographs of ephemeral streams in the Southwest: Am. Soc. Civil Engineers Proc., Hydraulics Div. Jour., v. 92, no. HY2, p. 33-52.
- Rubey, W. W., 1937, The force required to move particles on a stream bed: U.S. Geol. Survey Prof. Paper 189-E, p. 121-141.
- Schumm, S. A., and Lichty, R. W., 1963, Channel widening and flood-plain construction along Cimarron River in southwestern Kansas: U.S. Geol. Survey Prof. Paper 352-D, p. D71-D88.
- Sellers, W. D., ed., 1960, Arizona climate: Tucson, Arizona Univ. Press, 60 p.
- U.S. Geological Survey, 1961, Surface water supply of the United States, 1960—Part 9, Colorado River basin: U.S. Geol. Survey Water-Supply Paper 1713, 520 p.



